

Clinical quantitative coronary artery stenosis and coronary atherosclerosis imaging: a Consensus Statement from the Quantitative Cardiovascular Imaging Study Group

A list of authors and their affiliations appears at the end of the paper

Abstract

The detection and characterization of coronary artery stenosis and atherosclerosis using imaging tools are key for clinical decision-making in patients with known or suspected coronary artery disease. In this regard, imaging-based quantification can be improved by choosing the most appropriate imaging modality for diagnosis, treatment and procedural planning. In this Consensus Statement, we provide clinical consensus recommendations on the optimal use of different imaging techniques in various patient populations and describe the advances in imaging technology. Clinical consensus recommendations on the appropriateness of each imaging technique for direct coronary artery visualization were derived through a three-step, real-time Delphi process that took place before, during and after the Second International Quantitative Cardiovascular Imaging Meeting in September 2022. According to the Delphi survey answers, CT is the method of choice to rule out obstructive stenosis in patients with an intermediate pre-test probability of coronary artery disease and enables quantitative assessment of coronary plaque with respect to dimensions, composition, location and related risk of future cardiovascular events, whereas MRI facilitates the visualization of coronary plaque and can be used in experienced centres as a radiation-free, second-line option for non-invasive coronary angiography. PET has the greatest potential for quantifying inflammation in coronary plaque but SPECT currently has a limited role in clinical coronary artery stenosis and atherosclerosis imaging. Invasive coronary angiography is the reference standard for stenosis assessment but cannot characterize coronary plaques. Finally, intravascular ultrasonography and optical coherence tomography are the most important invasive imaging modalities for the identification of plaques at high risk of rupture. The recommendations made in this Consensus Statement will help clinicians to choose the most appropriate imaging modality on the basis of the specific clinical scenario, individual patient characteristics and the availability of each imaging modality.

✉ e-mail: dewey@charite.de

Sections

Introduction

Clinical need for imaging consensus

Method for generating consensus recommendations

Technical features and risks of imaging tools

Imaging modalities for stenosis assessment

CT for coronary atherosclerosis imaging

MRI for coronary atherosclerosis imaging

PET for coronary atherosclerosis imaging

ICA for coronary atherosclerosis imaging

IVUS for coronary atherosclerosis imaging

OCT for coronary atherosclerosis imaging

Conclusions

Consensus statement

Introduction

Given that quantitative imaging of coronary atherosclerosis and coronary artery stenosis has become widely available in the past 5 years, an interdisciplinary consensus on its role in clinical practice for the management of patients with suspected or known coronary artery disease (CAD) is highly desirable. During the Second Quantitative Cardiovascular Imaging (QCI) meeting on 9 September 2022, the current status and future potential of coronary atherosclerosis and stenosis imaging were discussed from the viewpoint of clinicians (radiologists, cardiologists and a cardiac surgeon), biomedical engineers and computer scientists. This multidisciplinary approach formed the basis of this Consensus Statement on the clinical appropriateness of various quantitative imaging modalities for coronary artery stenosis and atherosclerosis. In this Consensus Statement, we present the current clinical quantitative imaging techniques available for the direct visualization of coronary artery stenosis and atherosclerosis for the detection of CAD, selection of the best treatment strategy and improvement in procedural planning.

Clinical need for imaging consensus

The appropriate assessment of the severity of coronary artery stenosis and the extent of atherosclerotic burden is paramount for the selection of the most effective preventative measures and for guiding clinical decision-making in patients with known or suspected CAD. From a clinical perspective, three major questions need to be answered: What is the best imaging technique for direct confirmation of CAD? How can imaging help to identify the best treatment strategy? And, how can imaging improve procedural planning?

Direct confirmation of CAD

Imaging has a crucial role in the diagnosis of obstructive CAD. Although invasive coronary angiography (ICA) was the reference standard for imaging of obstructive CAD, several trials conducted in the past 6 years have compared the effectiveness of ICA versus CT in

patients with stable chest pain and found no significant difference in diagnostic performance between the two techniques for the identification of obstructive CAD, whereas CT identified more of the patients with non-obstructive CAD^{1–5}. In patients with stable chest pain and an intermediate pre-test probability of CAD, the DISCHARGE trial⁴ showed a lower rate of major procedural complications when CT was used as the initial imaging test instead of ICA to define subsequent management^{4,5}. According to findings from the RAPID-CTCA trial⁶, early coronary CT angiography in addition to standard of care did not improve clinical outcomes at 1 year compared with standard of care only in patients at intermediate risk of acute coronary syndrome (ACS) and subsequent clinical events. In contrast to CT, the role of other imaging modalities in the direct visualization of coronary stenosis has so far been investigated only in diagnostic studies⁷ and randomized trial data are lacking.

Identifying the best treatment strategy

Ideally, imaging would help to stratify patients who benefit from optimal medical treatment (OMT) and risk factor modification alone or from additional revascularization by either percutaneous coronary intervention⁸ (PCI) or coronary artery bypass graft (CABG) surgery^{9–11}. The ISCHEMIA trial¹² showed that invasive treatment (predominantly PCI) compared with OMT and risk factor modification did not prevent major adverse cardiovascular events (MACE) until a median of 3.2 years of follow-up in patients with obstructive CAD and moderate or severe ischaemia, highlighting the challenge of identifying patients who will benefit from revascularization. Furthermore, a large meta-analysis reported a lower risk of cardiac death in patients with stable CAD (particularly those with multivessel disease) who underwent revascularization compared with patients who received OMT only¹³. Multiple trials and an individual patient data meta-analysis of five trials that compared PCI with CABG surgery as the primary revascularization therapy in patients with multivessel disease showed a survival benefit and reduction in spontaneous myocardial infarction (MI) with CABG surgery^{14,15}, which might be related to the protection of distal vascular territories provided

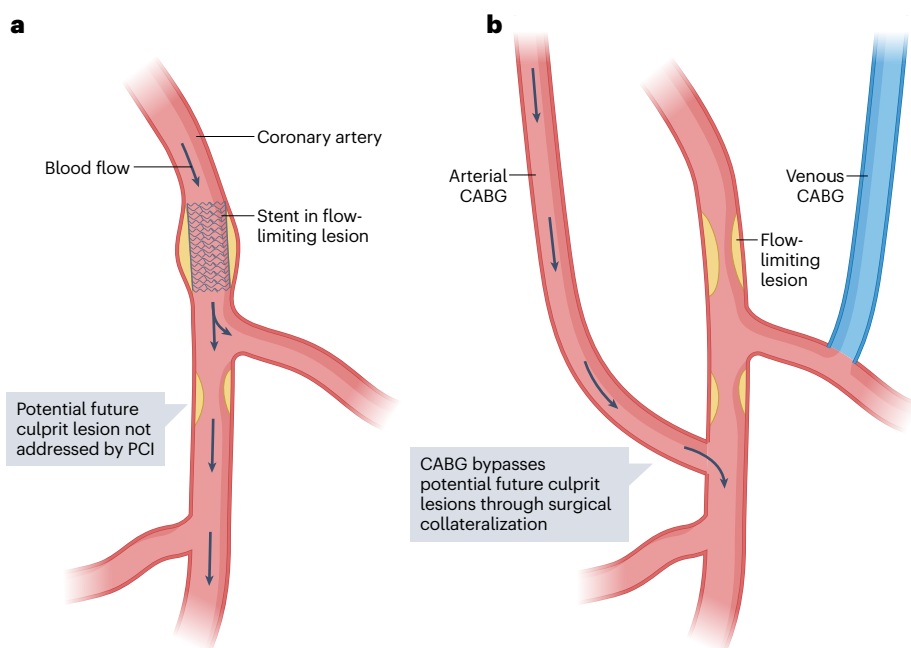


Fig. 1 | Main differences in the revascularization concepts between PCI and CABG surgery. a, Percutaneous coronary intervention (PCI) has the advantage of re-establishing coronary artery blood flow after angioplasty and stent placement in a flow-limiting lesion. However, potential non-obstructive culprit lesions downstream of the stent are not treated, which could lead to infarction in distal vascular territories. **b**, By contrast, coronary artery bypass graft (CABG) surgery provides a bypass for alternative blood supply to distal coronary territories (usually from an internal thoracic or radial artery or alternatively the saphenous vein), which has the advantage of protecting distal vascular territories because the grafts are usually inserted distally to additional plaque²¹.

Consensus statement

by surgery (Fig. 1). In addition, a network meta-analysis underscored the importance of OMT¹⁶. In patients with CAD without left main disease or a reduction in ejection fraction, OMT alone had the advantage of reducing the risk of stroke compared with CABG surgery but was associated with an increase in the rate of MI and all-cause death¹⁶.

Given that CABG surgery is most beneficial in patients with more severe CAD¹⁷, clinical quantitative coronary imaging for the assessment of atherosclerotic plaque burden is highly desirable. The original SYNTAX score was developed to help to select the best revascularization therapy for individual patients on the basis of anatomical distribution and complexity as well as the severity of stenosis as assessed on ICA¹⁷. To overcome the shortcomings of assessing only anatomical variables, comorbidities and other risk modifiers were included in the SYNTAX II score¹⁸. The SYNTAX II and SYNTAX II 2020 scores have not been validated in prospective trials; instead, they were used only in retrospective analyses involving the stratification of patients according to whether they would benefit most from CABG surgery or PCI^{19,20}. Therefore, testing the combination of clinical quantitative imaging with risk stratification would be pivotal in optimizing treatment to prevent MI, which is most commonly caused by the rupture of plaques without previous flow limitations^{21–23}. In addition to CT, two invasive imaging techniques that can identify high-risk plaque features are intravascular ultrasonography (IVUS) and optical coherence tomography (OCT)²⁴. In the PROSPECT study²⁵, a plaque burden of >70% measured by IVUS was associated with MACE during a follow-up period of 3–4 years. However, whether these imaging-assessed features could help to prevent events remains to be determined. Of note, only PET and, to some extent, MRI can detect coronary artery plaque inflammation, which is linked to plaque rupture and subsequent MI, and might therefore prompt more intensive OMT^{26,27} (Fig. 2).

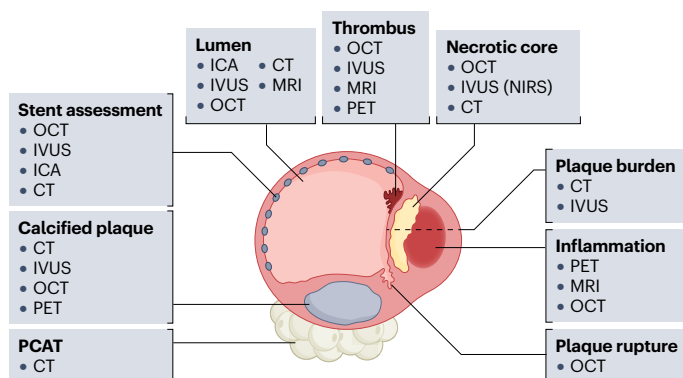


Fig. 2 | Targets of clinical coronary stenosis and atherosclerosis imaging. The figure shows a cross-section of a coronary artery and summarizes the different coronary stenosis and atherosclerosis imaging targets and the appropriateness of each imaging modality for each target on the basis of the Quantitative Cardiovascular Imaging group consensus. The appropriateness is shown in descending order for each of the imaging targets. CT is an appropriate modality to assess plaque burden, coronary plaque, coronary artery lumen dimensions (such as stenosis) and pericoronary adipose tissue (PCAT) and might facilitate the assessment of the necrotic core as low-attenuation plaque as well as coronary stents. MRI can be used to assess inflammation and thrombi in a research setting. PET is the best technology to detect and quantify coronary artery plaque inflammation and can also be used to identify coronary thrombi, albeit at a lower accuracy than with optical coherence tomography (OCT) or intravascular ultrasonography (IVUS). Invasive coronary angiography (ICA) is the reference standard to assess coronary lumen dimensions and basic stent characteristics. NIRS, near-infrared spectroscopy.

Improving procedural planning

Several trials have demonstrated that complete revascularization, which was mostly determined by non-quantitative visual estimation of coronary stenosis in epicardial vessels, can improve patient outcomes²⁸. The use of fractional flow reserve (FFR) measurements to guide the appropriate use of PCI was first introduced to limit the number of stents needed. Investigators in the FAME-3 trial⁹ compared this strategy with CABG surgery in patients with multivessel disease and established that, at 1 year, FFR-guided PCI was not found to be non-inferior to CABG surgery with regard to the incidence of a composite of death, MI, cerebrovascular accident or repeat revascularization. This finding gives rise to two important considerations. First, the optimal target lesion for PCI, whether it be a flow-limiting stenosis or a vulnerable plaque, remains to be determined. Second, CABG surgery-mediated revascularization, which is fundamentally different from PCI-mediated revascularization, effectively provides the heart with a new autologous network of collaterals and might be particularly beneficial for preventing future MI in patients with a high plaque burden and multiple vulnerable plaques (Fig. 1). Therefore, the extraction of quantitative data from coronary atherosclerosis imaging pertaining to geometry, stability, inflammatory status and total plaque burden²⁹ will be important not only to help decide whether CABG surgery or PCI is more appropriate but also to tailor the revascularization strategy to the individual patient^{27,30}.

Method for generating consensus recommendations

Progress in the field of coronary artery stenosis and atherosclerosis imaging requires experts from numerous specialties to identify appropriate clinical applications for the different techniques. The complexity of the different imaging modalities means that a comprehensive consensus is needed. We assembled the QCI group of experts comprised of a cardiac surgeon, ten radiologists, nine cardiologists, six biomedical engineers and scientists, and five computer engineers. The expert talks were held during the Second QCI Consensus Meeting at Charité – Universitätsmedizin Berlin on 9 September 2022. We used the Delphi method^{31,32} to generate and ask participants a set of 29 questions (Supplementary Table 1) in a total of 3 rounds.

The first Delphi round took place online 2 weeks before the QCI meeting. The participants received a personalized link to the questionnaire via the Welphi web application^{33,34}. The second round took place onsite during the meeting, after the expert talks. The third and final round took place online 3 weeks after the meeting. While answering each question, each participant was shown their answers from the previous round in the online tool and could revise this default answer when deemed appropriate (Supplementary Figs. 1 and 2). In addition, before the second and third round, anonymized interim results from all experts in the previous round were shown in the form of a boxplot that presented the median response for each question (Supplementary Table 1, Supplementary Figs. 3 and 4). A total of 29 questions were presented in five categories: general clinical characteristics of coronary artery stenosis and atherosclerosis imaging modalities (five questions), specific indications (eight questions), specific groups of patients (seven questions), specific coronary stenosis pathophysiology (three questions) and specific atherosclerosis pathophysiology (six questions) (Supplementary Table 1). The answers were entered using a Likert scale from 1–9, whereby a score of 1–3 meant inappropriate, 4–6 meant uncertain and 7–9 meant appropriate³⁵. The process was designed to present and weigh the advantages and disadvantages of

Consensus statement

General clinical characteristics	CT	MRI	PET	SPECT	ICA	IVUS	OCT
Availability of modality in clinical practice	9	6	4	5	9	6	5
Modality is commonly applied in clinical practice	8	5	2	4	9	5	4
Modality includes quantification in clinical practice	8	5	5	4	7	7	7
Cost-effectiveness of imaging technique	8	5	3	4	6	5	5
General adverse events profile	8	8	7	7	6	5	5

Specific indications	CT	MRI	PET	SPECT	ICA	IVUS	OCT
Stable chest pain with suspected CAD and intermediate pre-test probability (10–60%)	9	6	4	5	5	3	3
Stable chest pain with suspected CAD and high pre-test probability (>60%)	7	6	4	4	8	6	6
After an inconclusive or non-diagnostic functional test	8	5	4	4	7	5	5
ACS without ST-segment elevation	7	4	3	3	8	6	6
ACS with ST-segment elevation	3	2	1	1	9	7	7
Asymptomatic patients with a high risk of CVD (>10% risk of cardiovascular events in the subsequent 10 years)	7	4	2	2	2	2	2
New symptoms in patients with prior coronary stenting	7	5	4	5	8	6	6
New symptoms after CABG surgery	8	6	4	4	7	5	5

Specific groups of patients	CT	MRI	PET	SPECT	ICA	IVUS	OCT
Female patients	8	7	5	5	7	7	7
Young age (<55 years)	8	7	4	4	6	5	5
High heart rate (>70 bpm)	7	6	5	5	8	7	7
High BMI (>30 kg/m ²)	7	6	5	5	7	7	7
Valvular heart disease (including planned transcatheter aortic valve implantation)	9	6	3	2	7	5	4
After heart transplantation	8	6	4	4	7	6	6
Chronic kidney disease (GFR <30 ml/min/1.73 m ²)	6	6	5	5	6	5	5

Coronary artery stenosis imaging: physiological considerations	CT	MRI	PET	SPECT	ICA	IVUS	OCT
Coronary artery anatomy (including anomalies)	9	6	3	2	7	3	3
Accuracy of coronary artery stenosis measurement	8	5	2	1	8	8	9
Susceptibility of stenosis measurement to artefacts	6	5	4	4	7	7	6

Coronary atherosclerosis imaging: pathophysiological considerations	CT	MRI	PET	SPECT	ICA	IVUS	OCT
Coronary plaque morphology	8	5	2	1	5	8	9
Coronary plaque composition	8	5	2	1	3	8	8
Total coronary plaque burden	9	5	3	2	6	7	6
Culprit coronary plaque detection	7	5	4	2	7	8	8
Coronary plaque composition	6	5	7	2	2	5	6
Pericoronary adipose tissue	8	5	4	3	1	3	3

Appropriate
 Uncertain
 Inappropriate

Fig. 3 | Clinical characteristics and appropriateness of imaging modalities for coronary artery stenosis and atherosclerosis imaging. The values shown are the median ratings from the 31 experts for each of the 29 clinical questions asked during the three-round clinical Delphi process. ACS, acute coronary syndrome;

CABG, coronary artery bypass graft; CAD, coronary artery disease; CVD, cardiovascular disease; GFR, glomerular filtration rate; ICA, invasive coronary angiography; IVUS, intravascular ultrasonography; OCT, optical coherence tomography.

each modality with regard to different technical aspects and specific clinical indications, and individual participants influenced each other to gain a collective understanding of the subject discussed and to reach a consensus in a streamlined and consistent manner (Fig. 3).

Technical features and risks of imaging tools

A technical comparison of imaging tools is provided together with a risk assessment in Table 1, and a comparison of the technical challenges is shown in Table 2.

Non-invasive imaging modalities

CT has a high spatial and temporal resolution for non-invasive assessment of coronary stenosis and plaque composition^{36,37} (Figs. 4 and 5) within a single heartbeat using a protocol that exposes the patient to a low dose of radiation (3–5 mSv)^{38–40}. On the other hand, CT requires intravenous administration of a highly concentrated iodine-based contrast agent and is susceptible to artefacts from high heart rates or the presence of highly calcified coronary plaques⁴¹ (Fig. 2). Of note, intravenous contrast agents used for coronary CT angiography are associated with a lower rate of contrast-associated acute kidney injury (5.6%) than the intra-arterial contrast agent used during ICA (13.2%)⁴². Interestingly, in an intraindividual comparison of data from the CAD-Man trial⁴³, the rate of variations in physiological serum creatinine levels that met the definition of post-contrast acute kidney injury (2.2–2.6%) was similar to the rate of acute kidney injury 2 days after

undergoing coronary CT angiography (2.2%). The rate of major procedural complications of CT in the DISCHARGE trial (0.05%) was lower than the rate associated with ICA procedures without PCI (1.0%) and that of ICA with PCI (5.6%)⁴. In the DISCHARGE trial⁴, major procedural complications were fourfold lower in the CT-first group than in the direct-to-ICA group, even when complications that occurred after these diagnostic procedures were included⁴. This finding suggests that, in terms of risk assessment, the initial use of non-invasive coronary CT angiography is more advantageous than proceeding directly to ICA. In expert centres, coronary MRI techniques offer the option of a free-breathing examination without exposure to ionizing radiation but this tool cannot be used to assess smaller vessels^{26,44,45} and is currently available only in research settings^{26,44}. Available sequences on most MRI scanners can assess stenotic segments, plaque inflammation and acute thrombi, and the images generated by these scanners are not affected by artefacts produced by high-density calcium^{46–50} (Figs. 4 and 6). On the other hand, cardiac MRI is limited by long acquisition times and low spatial resolution in protocols designed for motion correction⁴¹. Importantly, claustrophobia occurs commonly during MRI (2% of outpatients and 10% of inpatients) and MRI-related safety risks might arise from the referral of patients with absolute contraindications (such as the presence of shrapnel), which occurs at a rate of 0.4%⁵¹. PET and SPECT are hybrid imaging modalities that, together with CT, provide the option of direct coronary imaging⁵². PET using ¹⁸F-sodium fluoride (¹⁸F-NaF) can facilitate the assessment of microcalcifications, whereas

Consensus statement

PET using ^{68}Ga -DOTATATE allows visualization of plaque inflammation, and PET using ^{18}F -glycoprotein 1 allows the assessment of thrombus^{52,53} (Fig. 7). The rate of adverse events associated with the use of radiopharmaceuticals, which includes cutaneous effects, such as rashes and skin flushing, and cardiovascular effects, such as hypotension and anaphylactoid reactions, is 2.1–3.1 per 100,000 administrations^{54,55}. The effective radiation dose of PET plus CT is approximately 10 mSv when combining radiation emitted by coronary CT angiography, attenuation correction CT and the radiotracer²⁷. The use of PET plus MRI can reduce radiation exposure to 4–5 mSv, and the wide field of view scanners might reduce this exposure level even further to <1 mSv. The assessment of small coronary vessels by PET alone is not possible

because of its low spatial resolution (~4 mm), the registration issues between PET and CT acquisitions, and potential motion artefacts^{56,57}. SPECT is predominantly used for imaging of myocardial ischaemia³⁵ and has a limited role in coronary plaque imaging in animal models⁵⁸.

Invasive imaging modalities

With its high temporal and spatial resolution, ICA is the reference standard for stenosis assessment⁵⁹ (Fig. 4). ICA is invasive in nature and involves the use of iodine contrast agents and exposure to ionizing radiation⁵⁹. As noted above, in the randomized CAD-Man trial⁴², the intra-arterial administration of contrast media for ICA resulted in a higher rate of contrast-associated acute kidney injury than intravenous contrast

Table 1 | Comparison of imaging tools for visualization of coronary stenosis and atherosclerosis

Imaging modality	Ionizing radiation	Contrast agent, tracer or non-contrast technique	Risk assessment	Temporal resolution (acquisition time per frame)	Spatial resolution (image analysis voxel size)	Penetration depth
CT	Median effective dose is ~2–5 mSv (refs. 67,155,156)	High iodine concentration (~350–400 mg/ml of iodine), intravenous administration with a significantly lower rate of AKI of 5.6% compared with ICA ⁴²	Only 0.05% of patients receiving CT in the DISCHARGE trial ⁴ had a major procedural complication related to CT assessment	150–200 ms	Axial resolution 0.35×0.35 mm ² with slice thickness: 0.5–0.7 mm	NA
MRI	No	Coronary MRI angiography: non-contrast-enhanced 3D bSSFP/T1-GRE sequence; coronary MRI plaque: motion-corrected RD; T1-GRE thrombus: MRDTI	Referral of patients with absolute contraindications (such as shrapnel or a pacemaker) can be a safety concern and occurs at a rate of 0.4% ²¹ ; claustrophobia is also common	20–60 ms	Coronary MRI angiography: 0.9–1.3 mm ³ ; coronary MRI plaque imaging: 0.8–1.5 mm ³	NA
PET	Effective dose of ~10 mSv for the combination of coronary CT angiography, attenuation correction CT and the radiotracer ^{157,158}	For plaque imaging: calcification (^{18}F -NaF); glucose metabolism (^{18}F -FDG); SSTR2 (^{68}Ga -DOTATATE)	Similar risks as noted for CT, plus the risks of the PET tracer; the incidence of radiopharmaceutical adverse events has been reported to be as low as 2.1–3.1 per 100,000 administrations ^{54,55}	5–10 s	Axial resolution: 3–5 mm	NA
SPECT	Yes, but not currently applicable to clinical coronary imaging	Currently NA for atherosclerosis assessment; stenosis can be assessed by the CT component of the procedure	Currently no clinical coronary imaging application	5 s to 10 min	Axial resolution: 6–10 mm	NA
ICA	Yes, with a median effective dose of 4.1 mSv (ref. 4)	Intra-arterial administration of an iodine contrast agent with a significantly higher rate of AKI of 13.2% compared with CT ⁴²	Major procedural complications occurred in 1.9% of the ICA group in the DISCHARGE trial ⁴ , which was significantly more frequent than in the CT group (0.5%)	1–10 ms	Axial resolution: 0.1–0.2 mm	NA
IVUS	Not by itself, but ionizing radiation is used during the ICA procedure	NA	IVUS involves the risks of ICA plus additional IVUS procedure-related risks; coronary vasospasm is the most common major procedural complication (incidence of ~3%) and pretreatment with nitrates is recommended ⁶⁶	30–100 frames per s	Axial resolution: 100–150 μm; lateral resolution: 150–300 μm	4–8 mm
OCT	Not by itself, but ionizing radiation is used during the ICA procedure	Need for clearing during pullbacks (contrast or eventually saline in CKD)	OCT involves the risks of ICA plus additional OCT procedure-related risks; the rate of major procedural complications is similar to that of IVUS ¹⁵⁹	180–200 frames per s	Axial resolution: 10–15 μm; lateral resolution: 20–90 μm	0.4–2.0 mm (depending on type of tissue at selected location)

Consensus on the technical assessment of imaging modalities compiled in this Table was accomplished using the Delphi method with ratings by ten investigators (one cardiologist, five radiologists, one dual certified cardiologist–radiologist, one nuclear medicine physician and two methodologists). ^{18}F -FDG, ^{18}F -fluorodeoxyglucose; AKI, acute kidney injury; bSSFP, balanced steady-state free precession; CKD, chronic kidney disease; ICA, invasive coronary angiography; IVUS, intravascular ultrasonography; MRDTI, magnetic resonance direct thrombus imaging; NA, not applicable; OCT, optical coherence tomography; RD, respiratory dynamics; SSTR2, somatostatin receptor 2; T1-GRE, T1-weighted gradient echocardiography sequence.

Consensus statement

Table 2 | Comparison of technical challenges of imaging modalities

Imaging modality	Susceptibility to artefacts	Small-vessel assessment	User dependency	Need for ECG gating	Need for sedation
CT	Medium	Medium	Low	Yes	No
MRI	Medium	Low	High	Yes	No
PET	High	Low	Low	Yes	No
SPECT	High	Low	Low	Yes	No
ICA	Low	High	Medium	No	Yes, conscious sedation possible
IVUS	Medium	Medium	High	No	Yes, conscious sedation possible
OCT	Medium	Medium	High	No	Yes, conscious sedation possible

ECG, electrocardiogram; ICA, invasive coronary angiography; IVUS, intravascular ultrasonography; OCT, optical coherence tomography.

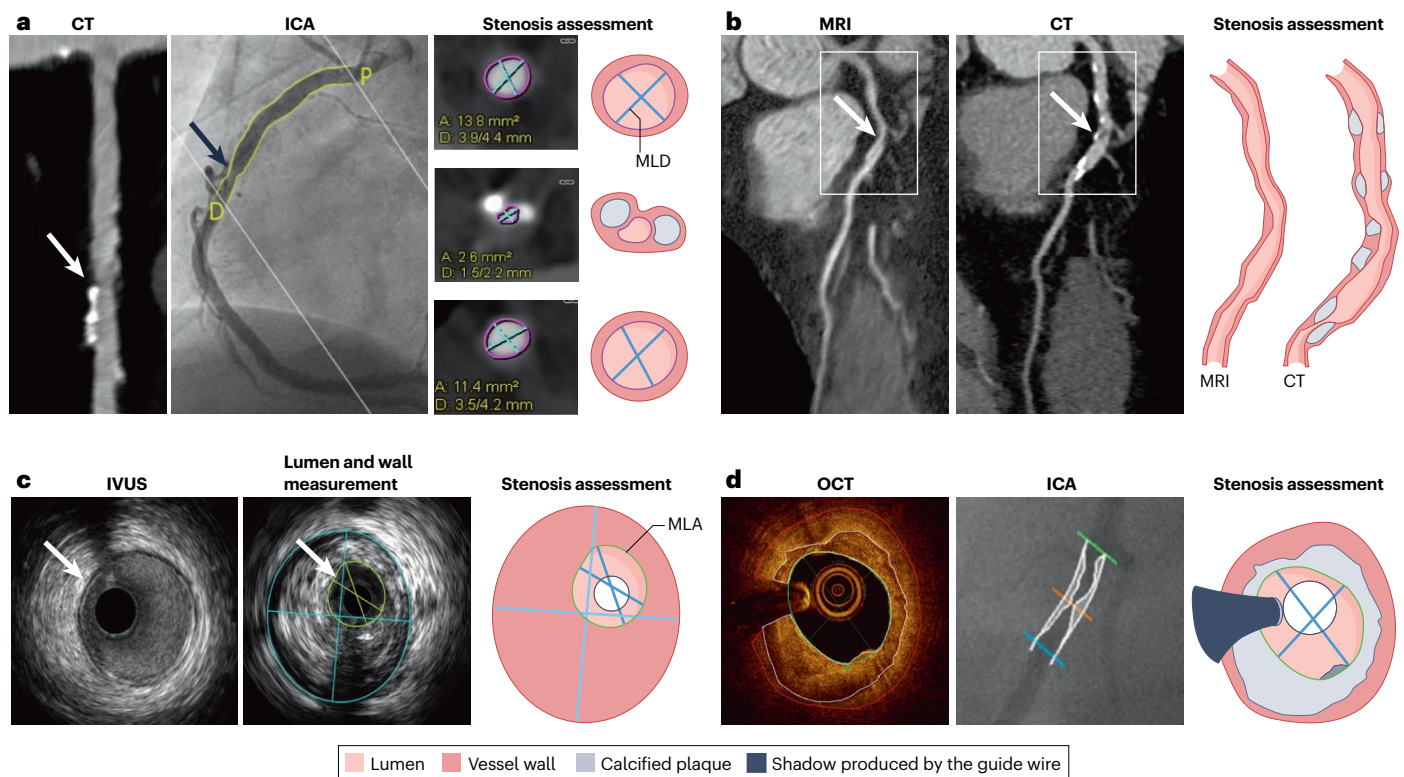


Fig. 4 | Imaging modalities for the assessment of coronary stenosis. **a**, CT obtained from a man aged 62 years with atypical chest pain and severe aortic stenosis. Straight reformation (left panel) of the right coronary artery (RCA) demonstrates several calcified plaques and a 40% diameter stenosis of the mid-RCA (arrow), which is confirmed by invasive coronary angiography (ICA; arrow in the middle panel). The severity of the stenosis (right panel) is based on the ratio of the minimal lumen diameter (MLD; blue line) and the average luminal diameter of the reference regions. **b**, MRI demonstrates a curved reformation (left panel) of the left anterior descending coronary artery. Both imaging modalities (MRI and CT) identified a >50% luminal diameter stenosis in the proximal left anterior descending coronary artery (arrows). The right panel demonstrates luminal dimension differences between MRI and CT. **c**, An intravascular ultrasonography (IVUS)-derived cross-sectional image of the RCA from an individual without coronary artery disease (left panel), with the IVUS catheter located centrally in the lumen. Note that, in normal coronary vessels, the wall is shown as a thin echogenic layer (arrow) delineated

by two low-echogenic layers that correspond to the intima and adventitia. In comparison, an obstructive coronary plaque in the RCA (middle panel) with a thickened wall causes a 50% diameter stenosis. Stenosis severity assessed by IVUS (right panel) can also be estimated as minimal lumen area (MLA; green line) or MLD (blue line); note that the high penetration depth of IVUS allows the visualization of the outer layers of the vessel wall. **d**, Cross-sectional optical coherence tomography (OCT) image from the mid-segment of the left circumflex coronary artery for assessment of an obstructive lesion with an 81% area stenosis and a 56% diameter stenosis (left panel). Quantitative ICA (middle panel) yields an area stenosis of 96% and a diameter stenosis of 79%, illustrating that lumen dimensions measured by OCT are larger and yield a less severe stenosis grade compared with the use of ICA⁷⁹. The graphical representation of the OCT axial image (right panel) compares the estimation of stenotic lesion based on MLA and MLD determined in the stenotic segment. D, distal; P, proximal.

Consensus statement

for CT. The rate of major procedural complications of ICA without PCI is approximately 20-fold higher than with CT (1.0% versus 0.05%)⁴. An important technical challenge of ICA is that vessel lumen dimensions

can be misrepresented owing to foreshortening and tortuosity⁵⁹. IVUS uses intra-coronary ultrasonography and has a lower spatial resolution but a higher penetration than OCT, allowing the assessment of plaque

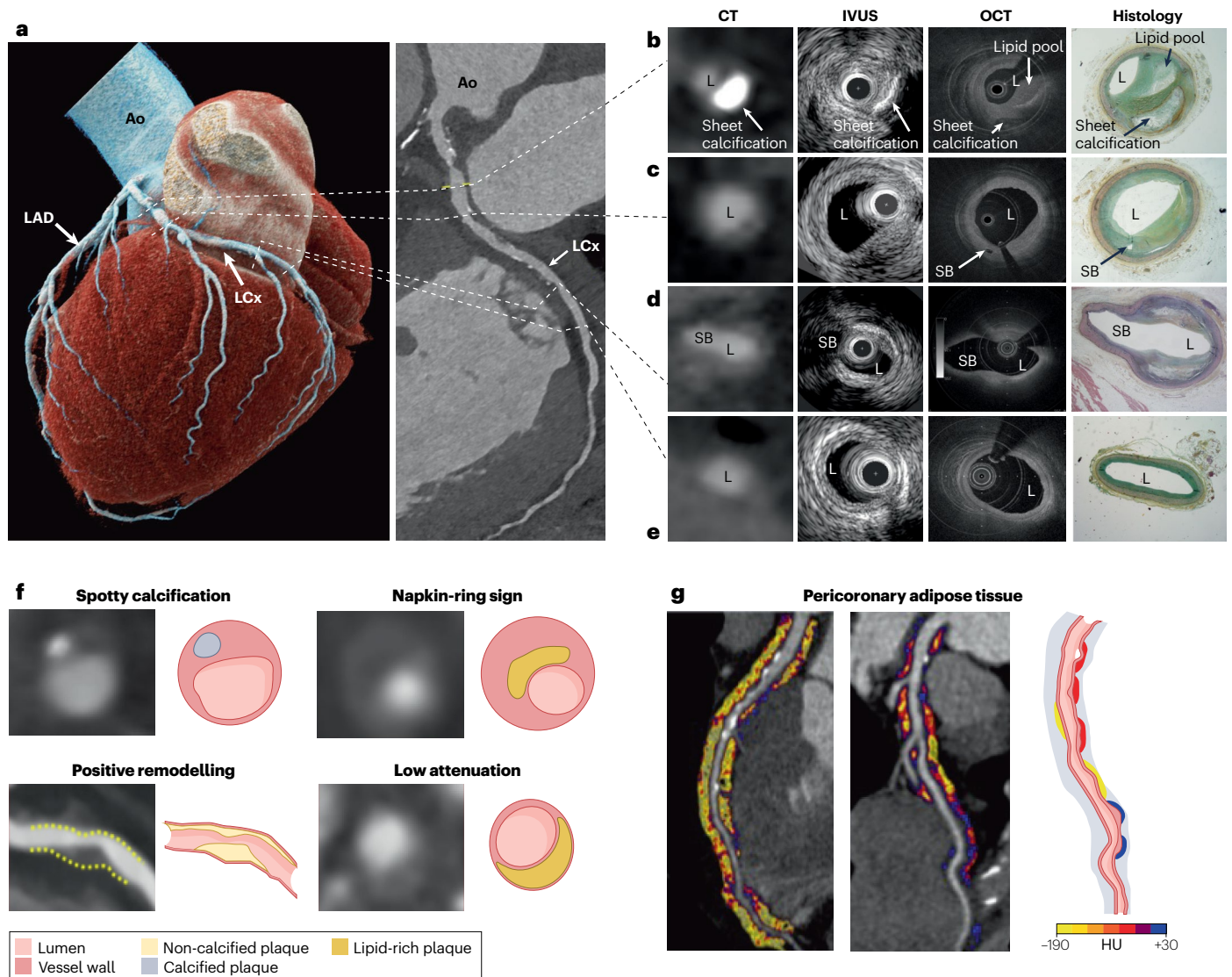


Fig. 5 | CT for quantitative coronary atherosclerosis imaging. Example of plaque characterization using CT angiography, intravascular ultrasonography (IVUS), optical coherence tomography (OCT) and histology. **a**, A volume-rendered (left panel) and a curved multiplanar reconstruction (right panel) of CT taken from a male patient aged 62 years with atypical angina using a photon-counting detector scanner with 0.2-mm slice thickness (part **a**). Parts **b–e** show cross-sectional correlations showing fibroatheroma with sheet calcification and lipid pool (part **b**), fibrous plaque and a small side branch (SB) (part **c**), early fibroatheroma and a large SB (part **d**), and adaptive intimal thickening (part **e**); derived from CT, IVUS, OCT and histology. These images were acquired as part of an ex vivo investigation (courtesy of Cardiovascular Imaging Research Center, Massachusetts General Hospital, Harvard Medical School, Boston, MA, USA). High-risk plaque features related to major adverse cardiovascular events depicted on CT (part **f**). Spotty calcification is a marker of ongoing inflammation: the image shows a cross-section of a partially calcified plaque (spotty calcification diameter <3 mm in all directions). Napkin-ring sign: the central area of the plaque adjacent to the

coronary lumen represents a lipid-rich core (low attenuation), which is surrounded by a peripheral rim of fibrous tissue in the vessel wall (higher CT attenuation). Positive remodelling of a non-calcified plaque: the dotted yellow lines indicate the vessel wall and show outward remodelling of the vessel wall at the location of highest plaque volume. Remodelling is calculated using vessel cross-sectional areas at the site of maximal stenosis or plaque divided by the average cross-sectional areas of proximal and distal reference segments, and an index of ≥ 1.1 is used to define positive remodelling. Low-attenuation plaque: a non-calcified plaque with an average attenuation of <30 Hounsfield units (HU). The napkin-ring sign, positive remodelling and low attenuation are associated with an increased risk of subsequent plaque rupture (Fig. 2). Pericoronary adipose tissue on CT has emerged as a strategy to detect and quantify coronary artery inflammation (part **g**). Pericoronary adipose tissue is shown using coloured attenuation maps around the right coronary, with a higher value (in terms of HU) indicating inflammation and a possible increased risk of disease in the future. Ao, aorta; L, lumen; LAD, left anterior descending coronary artery; LCx, left circumflex coronary artery.

Consensus statement

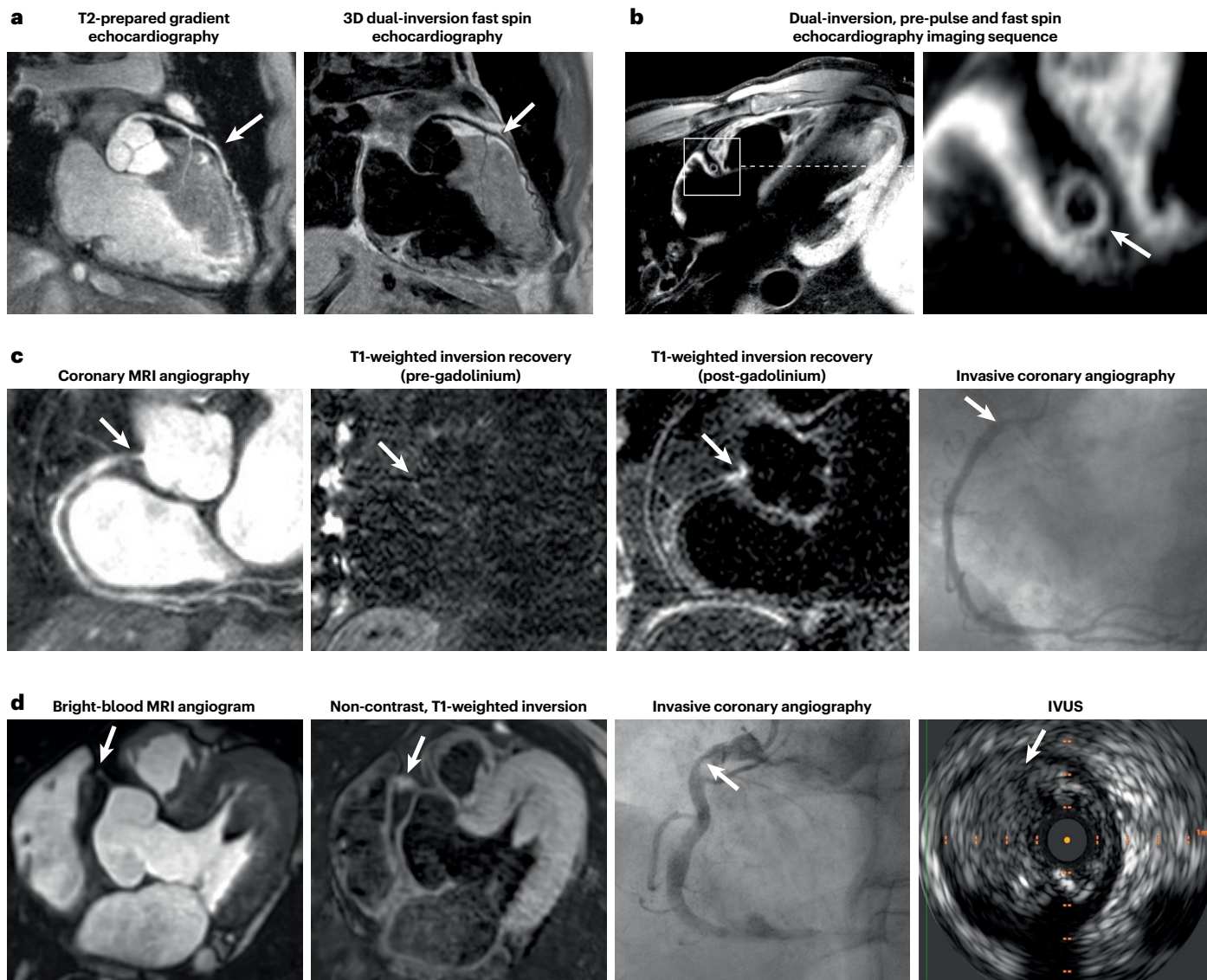


Fig. 6 | MRI for quantitative coronary atherosclerosis imaging. **a**, Contrast enhancement mechanisms in free-breathing 3D coronary MRI angiography. T2-prepared gradient echocardiography image (left panel) showing the left anterior descending coronary artery with high-intensity signal lumen (arrow). The same left anterior descending coronary artery is also visualized with a 3D dual-inversion fast spin echocardiography sequence (right panel), in which the lumen has low signal intensity (arrow). **b**, Coronary vessel walls can be assessed using a dual-inversion, pre-pulse technique in conjunction with a fast spin echocardiography imaging sequence (left panel). Magnification (right panel) of the right coronary artery (RCA) on an axial plane allows visualization of the coronary artery wall (arrow). **c**, Coronary MRI angiography (left panel) shows stenosis in the proximal RCA (arrow). The pre-contrast, inversion recovery image of the RCA (middle-left panel) shows no visible coronary enhancement (arrow).

However, the gadolinium-enhanced, inversion recovery image (middle-right panel) from the same anatomical location shows distinct signal enhancement in the area of the stenosis (arrow). Invasive coronary angiography confirms stenosis in the proximal RCA (right panel, arrow). **d**, The bright-blood MRI angiogram (left panel) shows a low-intensity signal stenosis in the proximal RCA (arrow), which has high intensity (arrow) in the simultaneous, interleaved and co-registered, non-contrast, T1-weighted inversion recovery sequence (middle-left panel) related to acute plaque rupture and thrombus (Fig. 2). The severity of the stenosis (arrow) is corroborated by invasive coronary angiography (middle-right panel) and shown as an acute intraluminal thrombus (arrow) on intravascular ultrasonography (IVUS) (right panel). Part a left-hand image adapted from ref. 160, Wiley; right-hand image adapted from ref. 161, Wiley.

composition, including plaque that affects all the layers of the vessel wall^{60–62} (Fig. 4). OCT uses near-infrared light with a high temporal and spatial resolution, but has a lower penetration depth than that of IVUS, which limits the evaluation of coronary plaque to 500 μm below the luminal surface^{62,63}. Both invasive intravascular modalities are limited

by their rigid probes in tortuous, stenotic, highly calcified, and small vessels⁶⁴ and have a role in the detection of clinically relevant stenosis and culprit lesions and in determining whether a plaque is at high risk of triggering future MACE⁶⁵. With regards to risk assessment, coronary vasospasm is the most common major procedural complication of

Consensus statement

IVUS and OCT (approximately 3%) and pretreatment with nitrates is recommended⁶⁶. Other major procedural complications of both IVUS and OCT, such as dissection, vessel occlusion or embolism, are rare (0.4%); of note, risk assessment for both these invasive intravascular modalities needs to include the risks of ICA (Table 1).

Imaging modalities for stenosis assessment

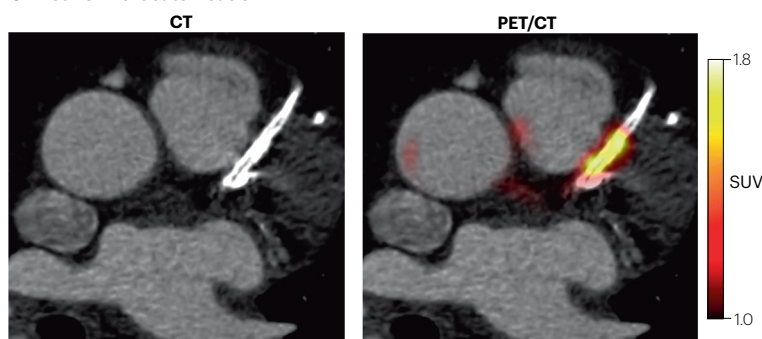
The results from our questionnaires on the most appropriate modality with regards to general patient characteristics, specific indications, patient groups and stenotic features are summarized in Fig. 3 and Supplementary Fig. 4. Meta-analyses have demonstrated that coronary CT angiography has an excellent sensitivity of 95–100% for the diagnosis of obstructive coronary artery stenosis compared with ICA as the reference standard^{67–69}. New-generation coronary MRI approaches have yielded an image quality that is similar to that of CT in selected patients^{70,71}. Although MRI is a promising modality for these patients, large, multicentre studies to compare its diagnostic accuracy with that of ICA or CT are not yet available. PET facilitates the detection of an increase in coronary plaque metabolism⁷² but, similar to SPECT, it

does not allow for the clinical assessment of coronary stenosis (Fig. 3). Historically, ICA was considered the reference standard for the assessment of stenosis severity and still has a role in identifying lesions that require immediate revascularization (>90% stenosis)⁷³. IVUS and OCT impose an additional procedural risk compared with ICA alone and are appropriate imaging modalities for patients with ACS and ST-segment elevation; however, the general cost-effectiveness of these techniques is uncertain^{74,75} (Fig. 3).

Quantitative assessment of stenosis

CT is appropriate for the measurement of the minimum lumen diameter and the minimum lumen area (MLA) of the stenosis, with the latter being a better measure of luminal narrowing in non-circular stenosis⁷⁶ (Fig. 4). CT is also most appropriate for women, young patients (aged <55 years) and individuals with a high BMI (>30 kg/m²) (Fig. 3). Coronary MRI is a potential option in expert centres for women and young patients and has an accuracy of 79% for the detection of obstructive CAD compared with ICA; however, MRI is not recommended for coronary stenosis measurement given its low spatial resolution and susceptibility to

a Active microcalcification



b Inflammation

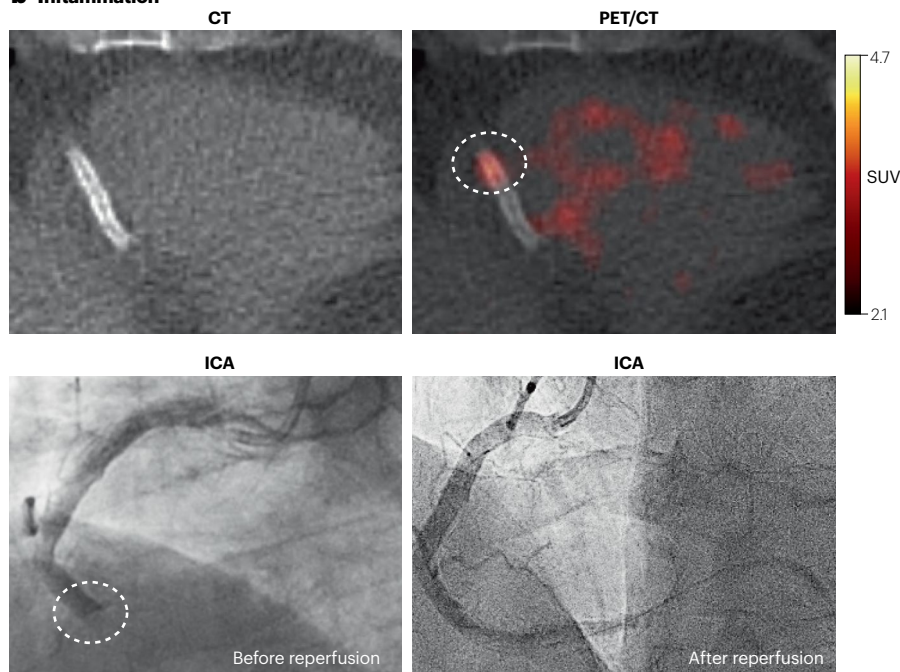


Fig. 7 | PET for quantitative coronary

atherosclerosis imaging. **a**, Demonstration of active microcalcification using ¹⁸F-NaF PET. Images taken from the PREFFIR trial¹³⁰ show active microcalcification in culprit, stented plaque in the left anterior descending coronary artery. The CT image (left panel) shows the stent in the left anterior descending coronary artery without a visible abnormality, whereas the PET/CT image (right panel) shows a focal site of increased active mineral deposition (Fig. 2). **b**, The panel shows the detection of C-X-C chemokine receptor type 4 (CXCR4)-positive inflammatory cells. CT and fused CXCR4-targeted PET/CT of a culprit stented lesion in acute ST-segment elevation myocardial infarction are shown. An elevated CXCR4 signal (top right panel, dashed circle) representing CXCR4⁺ inflammatory cell infiltrate¹³⁴ can be observed; the corresponding invasive coronary angiography (ICA) images show the culprit lesion before (bottom left panel, dashed circle) and after (bottom right panel) reperfusion. SUV, standard uptake values.

Consensus statement

artefacts²⁶ (Fig. 3). Owing to the lack of studies evaluating the accuracy of the CT component of PET and SPECT, both imaging modalities are currently considered inappropriate for stenosis quantification.

ICA has a high accuracy in measuring stenosis but is associated with substantial inter-observer variability⁷⁷, which can be improved with the use of quantitative coronary angiography⁷⁸, whereas ICA is preferable to CT in patients with a high heart rate. Stenosis quantification by IVUS and OCT can be performed with absolute (such as MLA) and relative measures (such as percentage area stenosis) (Fig. 4). Both invasive modalities are appropriate for stenosis measurement with low susceptibility to artefacts, whereas the size of the probes prevents the assessment of distal and very stenotic segments. Although the average luminal diameter measured by IVUS and, especially, OCT is generally larger than that measured on ICA⁷⁹, the measurements correspond well with actual dimensions from phantom models (measured diameter between -2.9% and 8.0%) and are highly reproducible^{79,80}.

Indications and clinical applications

CT is the most appropriate modality for assessing coronary anatomy in patients with stable chest pain with low-to-intermediate pre-test probability and is the preferred choice after heart transplantation^{4,81,82} (Fig. 3). The clinical indications for coronary MRI are currently uncertain because of a lack of randomized trial data⁸³. The high negative predictive value of coronary MRI in expert centres makes it a potential non-invasive, second-line option for direct coronary assessment in patients with low-to-intermediate pre-test probability⁸³. The general appropriateness of PET and SPECT remains uncertain.

The DISCHARGE trial⁴ and smaller randomized trials⁵ reported several benefits of a treatment strategy guided by CT instead of ICA in patients with stable chest pain and intermediate pre-test probability of disease. ICA remains the most appropriate imaging modality for direct coronary assessment in patients with stable chest pain and a high pre-test probability. ICA is also the most appropriate modality for patients with ACS, and the additional use of IVUS or OCT is considered appropriate if ST-segment elevation is also present. However, a meta-analysis has revealed that the use of different MLA cut-off values with IVUS and OCT, compared with FFR, has only moderate accuracy for the identification of haemodynamically significant stenosis^{84,85}.

Future directions

Improvements in the in-plane spatial resolution of CT from 0.35 mm to 0.16–0.25 mm (ref. 86) will reduce blooming artefacts, resulting in more accurate stenosis quantification and better lumen visualization in the presence of coronary stent struts⁸⁷. For MRI, advances in automated trigger delay determination, scan planning and image reconstruction will enable adequate spatial resolution within a single breath-hold⁸⁸. Automated calibration and lumen contouring in ICA can increase its applicability for quantitative assessment of stenosis, whereas imaging-derived computational flow indices for IVUS and OCT will facilitate an improvement in the identification of haemodynamically significant stenosis compared with luminal measurements alone^{89,90}.

Key points for stenosis assessment

- CT is the most appropriate modality as an initial test for the diagnosis of CAD in patients with stable chest pain and low-to-intermediate clinical likelihood of obstructive CAD.
- Coronary MRI does not expose the patient to ionizing radiation and can be a second-line option for direct coronary assessment in patients with stable chest pain and low-to-intermediate pre-test probability.

- ICA is the most appropriate test in patients with ACS and with stable chest pain and high pre-test probability.
- PET and SPECT have no role in the direct assessment of stenosis severity.
- IVUS and OCT are preferred in patients with ACS with ST-segment elevation and for planning stent placement.

CT for coronary atherosclerosis imaging

CT provides both qualitative and quantitative information on total coronary plaque burden and composition (Fig. 3 and Supplementary Fig. 4). Specifically, CT facilitates the detection and quantification of calcified, non-calcified and partially calcified plaque (Fig. 2) as well as the identification of high-risk plaque features^{91,92} (Fig. 5).

Quantitative assessment of atherosclerosis

Coronary artery calcium (CAC) plaque burden is quantified using the Agatston, volume or mass CAC scores^{93,94}. Given that the CAC score is a strong and independent predictor of cardiovascular events^{95,96}, this surrogate marker is recommended by guidelines for the refinement of 10-year risk stratification⁹⁷. In the SCOT-HEART trial⁹⁸, low-attenuation plaque burden (defined as <30 Hounsfield units) of >4% on CT was the strongest predictor of fatal and non-fatal MI in patients with stable chest pain (HR 4.65, 95% CI 2.06–10.5; $P < 0.001$). Plaque morphology measured on CT can also provide further prognostic information⁹⁹. In addition to a CAC score of ≥ 400 (refs. 4, 100), other high-risk coronary plaque features measured on CT include low attenuation, positive remodelling, napkin-ring sign and spotty calcifications^{91,92} (Fig. 5).

Indications and clinical applications

CT is the most appropriate modality for the quantification of total coronary plaque burden and for the assessment of coronary plaque morphology and composition. CT is also appropriate for culprit coronary plaque detection but was not rated as high as IVUS and OCT for this indication¹⁰¹ (Fig. 3). In asymptomatic individuals at an intermediate risk of CAD, CAC scoring, based on non-contrast CT, can add prognostic value beyond clinical risk factors and can guide decision-making regarding risk factor modification¹⁰⁰. Coronary plaque assessment using CT is visually intuitive and can be directly explained to patients and, therefore, might improve adherence to medical therapy and lead to more statin therapy recommendations¹⁰². Analysis of pericoronary adipose tissue surrounding the coronary arteries on CT has emerged as a new approach for the detection and quantification of coronary artery inflammation¹⁰³ via its capacity to measure a higher attenuation as an indirect biomarker of molecular and cellular changes¹⁰¹ (Fig. 5).

Future directions

The development of new software for CT scanners will allow rapid and fully automated quantification and characterization of the plaque in the whole coronary tree, which might ultimately be used as a support tool for routine clinical decision-making¹⁰⁴. In addition, further research on pericoronary adipose tissue will provide more insights into its possible clinical utility as a disease biomarker^{105,106}.

Key points for CT

- The spatial resolution of CT allows for quantitative assessment of coronary plaque with respect to dimension, composition, location and related risk of future cardiovascular events, making it the most appropriate modality for the quantification of total coronary plaque burden.

Consensus statement

- Increased and/or irregular heart rates, extensive coronary calcifications and the presence of coronary stents can hinder the evaluation of coronary atherosclerosis using CT.
- Automated whole-tree coronary plaque software, together with the higher temporal and spatial resolution provided by new CT scanners, will facilitate accurate quantification of coronary atherosclerosis.

MRI for coronary atherosclerosis imaging

Black-blood imaging sequences¹⁰⁷ are used to assess the lumen and vessel wall and to detect wall thickening as a marker of positive remodelling^{108–111} (Fig. 6). Dark-blood T1-weighted imaging detects hallmarks of plaque haemorrhage and luminal thrombi as hyperintense signals, which indicate the formation of methaemoglobin 12–72 h after a haemorrhagic event¹¹² (Fig. 6 and Supplementary Fig. 4). Furthermore, intraplaque inflammation (Fig. 2) and extracellular expansion related to angiogenesis have been targeted using contrast-enhanced, T1-weighted imaging after administration of a gadolinium-based contrast agent, and the results demonstrate a correlation between dynamic and late-signal enhancement and the severity of atherosclerosis¹¹³ (Fig. 6).

Quantitative assessment of atherosclerosis

High signal intensity of coronary plaque on non-contrast MRI, which correlates with a higher likelihood of unstable plaque¹¹⁴, can be quantified on T1-weighted inversion recovery images. Intriguingly, the extent of high-intensity plaque has been found to decrease after statin therapy¹¹⁵. The predominant substrate for these high-intensity plaques in stable CAD has been shown to be intraplaque haemorrhage but not lipids, which is in agreement with findings from near-infrared spectroscopy IVUS and indicates how MRI can contribute to the guidance and monitoring of therapy¹¹⁶.

Indications and clinical applications

The appropriate clinical use of MRI remains uncertain, given its limited resolution and 3D coverage (Fig. 3). Black-blood and dark-blood MRI might become alternatives to CT for the non-invasive assessment of coronary atherosclerosis¹¹⁷. The imaging of high-risk plaque features using MRI might help to better stratify risk and improve personalized medicine.

Future directions

The spatial resolution of MRI can be improved with the use of 3D imaging with isotropic voxel sizes of 0.8–1.5 mm and acquisition times of 10–15 min (refs. 41,48). The imaging signal can be improved by administering targeted gadolinium-based or iron-based contrast agents¹¹⁸. Alternatively, fluorine-based imaging agents might also improve contrast given the absence of a background signal¹¹⁹. Additional efforts to boost resolution include non-rigid motion correction for signal acquisition during extended periods of the cardiac cycle¹²⁰.

Key points for MRI

- MRI allows visualization of wall thickness, intraplaque haemorrhage and luminal thrombi as high-risk coronary plaque features but is limited by motion artefacts.
- MRI is currently not appropriate for use in clinical practice given its low resolution and lack of 3D coverage in comparison to CT.
- New technology to improve spatial resolution and motion correction as well as new contrast agents might allow MRI to be an appropriate non-invasive alternative to CT in the future.

PET for coronary atherosclerosis imaging

PET allows the assessment of disease activity in coronary plaque and research has focused largely on its role in the detection of coronary inflammation, calcification and thrombosis^{27,121,122} (Fig. 2). Radiotracers specifically targeting inflammation can be administered to identify and characterize distinct phases of inflammation¹²³ such as the targeting of glucose metabolism in activated macrophages with ¹⁸F-fluorodeoxyglucose (¹⁸F-FDG)¹²², the expression of the C-X-C chemokine receptor type 4 (CXCR4) on leukocytes and polarized macrophages¹²³, the expression of the somatostatin receptor subtype 2 in pro-inflammatory macrophages with ⁶⁸Ga-DOTATATE¹²⁴, and calcification activity using the ¹⁸F-NaF radiotracer¹²⁵ (Fig. 7).

Quantitative assessment of atherosclerosis

Most studies on the use of PET for the quantitative assessment of atherosclerosis have been conducted with the ¹⁸F-NaF radiotracer, which has been validated as a marker of calcification and disease activity using histology as the reference standard²⁷ (Fig. 7). The uptake of ¹⁸F-NaF is closely associated with disease progression and a change in CAC scores¹²⁶. Importantly, baseline ¹⁸F-NaF levels can help to identify the culprit plaque, whereas total coronary microcalcification activity can independently predict subsequent fatal or non-fatal MI¹²⁵.

Indications and clinical applications

PET is considered the most appropriate imaging modality for the assessment of coronary plaque inflammation (Fig. 3 and Supplementary Fig. 4) but remains primarily a research tool. ¹⁸F-FDG PET is already used to monitor the pharmacological modulation of inflammation in extra-coronary atherosclerotic plaques in clinical trials assessing novel anti-inflammatory drugs^{127,128}. Moreover, PET has provided insights into plaque pathobiology^{121,129}. Results from the prospective, multicentre, non-randomized PREFFIR study¹³⁰ confirmed the capacity of ¹⁸F-NaF PET to predict subsequent MI¹²⁵ and cardiovascular death in patients with advanced multivessel CAD and a history of recent MI. These findings can help identify patients with active disease states who might benefit from intensive pharmacotherapy (such as PCSK9 or IL-1 inhibitors).

Future development

New tracers will facilitate more specific interrogation of coronary inflammation and other key processes such as fibrosis¹³¹ and thrombus formation¹³². Advances in PET detector technologies will also improve the resolution and, therefore, increase the sensitivity of the modality for detecting disease progression¹³³. Finally, image processing solutions to address motion artefacts can markedly improve image quality and are becoming more widely available for clinical use¹³⁴.

Key points for PET

- PET is considered the most appropriate imaging modality for quantifying coronary plaque inflammation but, given its susceptibility to motion artefacts and its limited temporal and spatial resolution, PET is currently used only as a research tool.
- Technical advances and software updates will improve motion correction and overcome the limited spatial and temporal resolution of PET imaging.
- The use of ¹⁸F-NaF PET to measure calcification activity can help predict subsequent disease progression and event risk and has the potential to improve risk stratification and the identification of patients who require more intensive therapy.

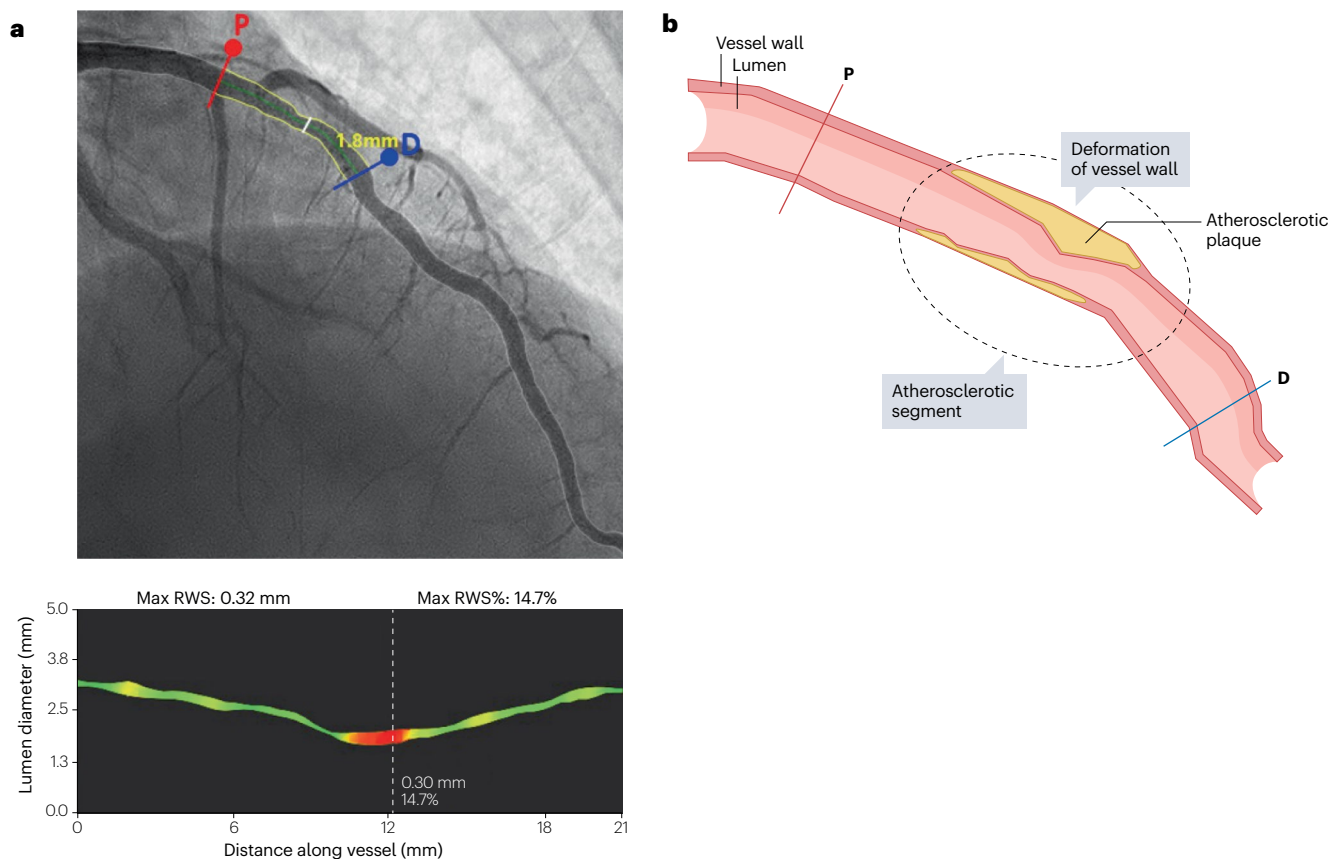


Fig. 8 | Representative example of coronary radial wall strain analysis. **a**, Invasive coronary angiography (ICA) shows a moderate lesion in the left anterior descending coronary artery (upper panel). Radial wall strain (RWS) is estimated using a single ICA projection with minimal lesion overlap and vessel foreshortening. To calculate RWS, first, the lumen diameter change along the target vessel during four representative phases of the cardiac cycle (end-diastole, early-systole, end-systole and end-diastole) is measured, where lumen diameter change is computed as the maximal diameter minus the minimal diameter over the cardiac cycle. RWS is then calculated as the lumen diameter change divided by the maximal diameter. The lower panel shows RWS along the length of the vessel of interest, where the dashed white line indicates the region with the highest RWS. A maximum RWS of >12% was

suggested as the threshold for defining vulnerable plaque on coronary radial wall strain analysis¹³⁵. RWS derived from ICA images correlates with invasive imaging-derived characteristics of plaque vulnerability such as the presence of thin-cap fibroatheroma. **b**, RWS for the assessment of atherosclerosis. RWS is a direct representation of the interaction between pulsatile coronary blood pressure and the composition of the vessel wall. Greater deformation of the vessel wall during the cardiac cycle corresponds to regions of high strain; of note, the most atherosclerotic segments (dashed circle) have a higher RWS. Vulnerable plaques tend to have higher RWS values and are more susceptible to rupture because of their higher biomechanical stress. D, distal; P, proximal.

ICA for coronary atherosclerosis imaging

ICA is the reference standard for the diagnosis of obstructive CAD⁴ but has a limited role in the direct visualization of coronary atherosclerosis (Fig. 3 and Supplementary Fig. 4).

Quantitative assessment of atherosclerosis

ICA detects the presence of atherosclerotic plaque on the basis of the imprint left on the vessel contour and, therefore, provides limited information on plaque morphology and composition (Fig. 3). Nonetheless, deformation of the vessel wall by circumferential tensile stress from pulsatile arterial pressure is directly dependent on tissue stiffness and, therefore, on plaque composition (Fig. 8). This deformation of the coronary artery, termed radial wall strain (RWS), can be measured on ICA, thereby expanding its clinical applicability¹³⁵.

Indications and clinical applications

ICA is appropriate for culprit coronary plaque detection (Fig. 3). As supported by our Delphi results, ICA is appropriate in patients with a high pre-test probability of CAD. Moreover, ICA is also indicated if a patient remains symptomatic despite guideline-directed medical treatment and in patients with CAD with high-risk anatomy (namely those with three-vessel disease or left main or proximal left anterior descending coronary artery stenosis)¹³⁶ (Fig. 3 and Supplementary Fig. 4).

Future directions

Promising ICA-based techniques that can assess coronary atherosclerosis, such as measurement of RWS, should be further explored¹³⁵. An additional ICA-derived parameter that can be used to stratify patients with CAD is endothelial shear stress, which can pinpoint regions of the

Consensus statement

coronary artery that are prone to developing plaques on the basis of computational fluid dynamics^{22,137}.

Key points for ICA

- ICA is appropriate for the detection of culprit coronary plaque, especially in patients with ACS, but does not permit direct visualization of the vessel wall and plaque composition.
- Coronary RWS is indirectly determined by coronary plaque composition and could have potential clinical applicability (Fig. 8).
- ICA is appropriate in patients with stable chest pain and a high pre-test probability of CAD (>60%).

IVUS for coronary atherosclerosis imaging

IVUS can characterize the morphology and composition of coronary artery plaque with a much higher penetration depth (4–8 mm) than that of OCT (0.4–2.0 mm)⁷⁵ but lower spatial resolution. IVUS allows visualization of all three layers of the coronary vessel wall and the detection of high-risk plaques that can reduce the effectiveness of PCI (Fig. 9).

Quantitative assessment of atherosclerosis

Positive remodelling is a common finding in early atherosclerosis that can be detected using IVUS and is associated with plaque rupture and thrombus formation¹³⁸ (Fig. 2). In the PROSPECT study²⁵, IVUS-based determination of a plaque burden of >70% in patients with ACS was associated with MACE caused by a non-culprit lesion during a follow-up of 3–4 years. IVUS probes that integrate near-infrared spectroscopy allow the detection and quantification of lipid-rich plaques with a maximum 4-mm lipid-core burden index of ≥ 400 , which was found to help with identifying patients at high risk of subsequent MACE during the 24-month follow-up¹³⁹. However, artefacts such as posterior shadowing in calcified plaque, reverberation and non-uniform rotational distortion can diminish coronary plaque visualization by IVUS¹⁴⁰ (Fig. 9).

Indications and clinical applications

IVUS is appropriate for the assessment of coronary plaque composition and the detection of culprit plaque (Fig. 3 and Supplementary Fig. 4). IVUS is considered less appropriate than CT for estimating total plaque burden and less appropriate than PET for assessing coronary plaque inflammation. IVUS is also useful for the identification of stent failure, particularly by determining malapposition, underexpansion and edge dissection⁶⁵ (Fig. 9). In the ULTIMATE trial¹⁴¹, the use of IVUS during the implantation of drug-eluting stents reduced the rate of cardiovascular death compared with the use of ICA alone.

Future directions

Current research on IVUS is focused on improving the automatic detection and measurement of coronary plaque^{142,143}. IVUS technologies that incorporate other imaging modalities (OCT or near-infrared spectroscopy) and the estimation of FFR will improve the identification of high-risk coronary plaques and their haemodynamic repercussions, respectively^{65,75}.

Key points for IVUS

- IVUS is appropriate for the assessment of coronary plaque composition and detection of culprit coronary plaque.
- The assessment of target vessels before stent implantation and the detection of stent failure are important clinical

applications of IVUS that will benefit from advances in automated detection and quantification of coronary plaque.

- The potential detection of superficial lesions with a high risk of rupture is an important area of IVUS research that can ultimately improve its clinical applicability, closer to that of OCT.

OCT for coronary atherosclerosis imaging

OCT is an invasive imaging modality that provides real-time tomographic views of coronary plaque at a very high resolution by using infrared light and fibreoptic technologies⁶⁵. OCT has the highest spatial resolution of all imaging modalities for the assessment of superficial coronary plaque lesions but has a lower penetration depth than that of IVUS⁶⁵. This low penetration depth also precludes the assessment of total coronary plaque burden by OCT. When used to assess suspected stent failure, OCT can detect uncovered struts, distinguish neoatherosclerosis from neointima, and identify thrombus and is more accurate in revealing stent underexpansion, malapposition and edge dissection than IVUS^{144–146} (Fig. 10).

Quantitative assessment of atherosclerosis

OCT can differentiate between the different phenotypes of culprit coronary plaque and can identify a thin-cap fibroatheroma (cap thickness <65 μm)^{63,147} (Fig. 10). Moreover, OCT can measure the thickness of the fibrous cap⁶³, identify high-risk plaques^{64,148} and macrophages (Fig. 10), and quantify plaque extension¹⁴⁹.

Indications and clinical applications

Given its high spatial resolution, OCT is the most appropriate modality for the assessment of coronary plaque morphology and is equally as appropriate as IVUS for the determination of coronary plaque composition and for culprit coronary plaque detection (Fig. 3 and Supplementary Fig. 4). The detailed visualization of luminal superficial lesions on OCT allows the identification of underlying causes of MI with non-obstructive coronary arteries such as spontaneous coronary artery dissection or embolic disease⁶⁴. In the ILUMIEN III: OPTIMIZE PCI trial¹⁵⁰, OCT-guided PCI achieved higher stent expansion (measured as minimum stent area) than ICA-guided PCI but was not superior to IVUS-guided PCI.

Future directions

Automated identification and quantification of coronary plaques by OCT is a focus of numerous ongoing studies^{151,152}. Combining OCT with other intravascular imaging modalities (such as IVUS and near-infrared spectroscopy) and OCT-based FFR might allow a more comprehensive assessment of coronary plaque and the effects on blood flow after stent implantation compared with the use of OCT alone^{148,153,154}. This improvement might in turn facilitate better identification of plaques with a higher risk of complications.

Key points for OCT

- OCT has high spatial resolution and therefore allows accurate assessment of superficial lesions but its penetration depth is lower than that of IVUS.
- The main challenges of OCT include its invasive nature, the expertise required to interpret images and its limited penetration depth.
- OCT is recommended to guide and optimize stent placement, especially in patients with complex lesions and anatomy.

Consensus statement

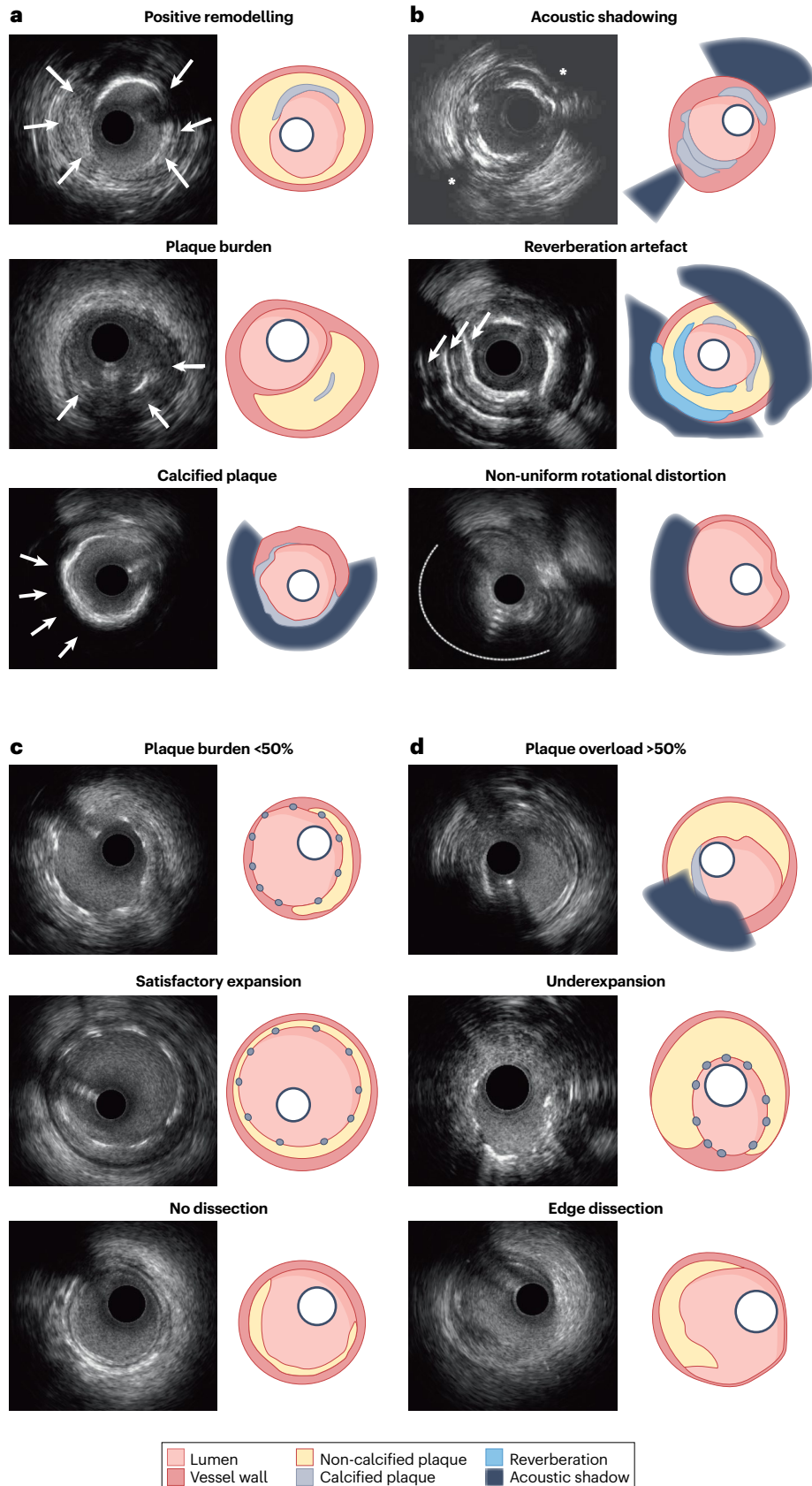


Fig. 9 | IVUS for quantitative coronary atherosclerosis imaging. Intravascular ultrasonography (IVUS) plaque detection and quantification. **a**, Positive remodelling is the thickening of the vessel wall secondary to coronary plaques (Fig. 2); in this example, the thickened wall (arrows) has already narrowed the vessel lumen (top panel). Plaque burden is calculated as the ratio of the atheroma area to the external elastic lamina of the vessel (arrows); the atheroma area is calculated by the difference between the external elastic lamina area and the lumen area (middle panel). Calcified plaque (arrows) causes acoustic shadowing, obscuring the external layers of the vessel wall (bottom panel). **b**, IVUS artefacts. Differentiating artefacts from true structures in IVUS is pivotal for plaque assessment. Acoustic shadowing behind calcific plaque (asterisks; top panel). Reverberation artefact can be seen as multiple equidistant reflections from calcium (arrows; middle panel). Non-uniform rotational distortion is seen along the curved dotted line (bottom panel). **c**, Optimal stent implantation by IVUS guidance. For optimal stent implantation (Fig. 2), the following criteria must be met: a plaque burden of <50% at 5 mm proximal or distal to the plaque edge (top panel), stent expansion at the minimal lumen area must be >5.0 mm² or 90% of the minimal lumen area of the reference segments (middle panel), and no dissection of >3 mm involving the media¹⁴¹ (bottom panel). **d**, Criteria for stent failure are plaque overload of >50% (top panel), underexpansion (middle panel) and edge dissection (bottom panel).

Consensus statement

Conclusions

Several modalities are available for clinical quantitative coronary artery stenosis and atherosclerosis imaging. CT is an accurate and reliable modality for stenosis assessment and quantification of total coronary

plaque volume, making it most appropriate for directing treatment in patients with stable chest pain and an intermediate pre-test probability of CAD²⁹. Even though MRI is currently not widely used in the clinical setting and is mostly used at expert centres, it has the potential to become

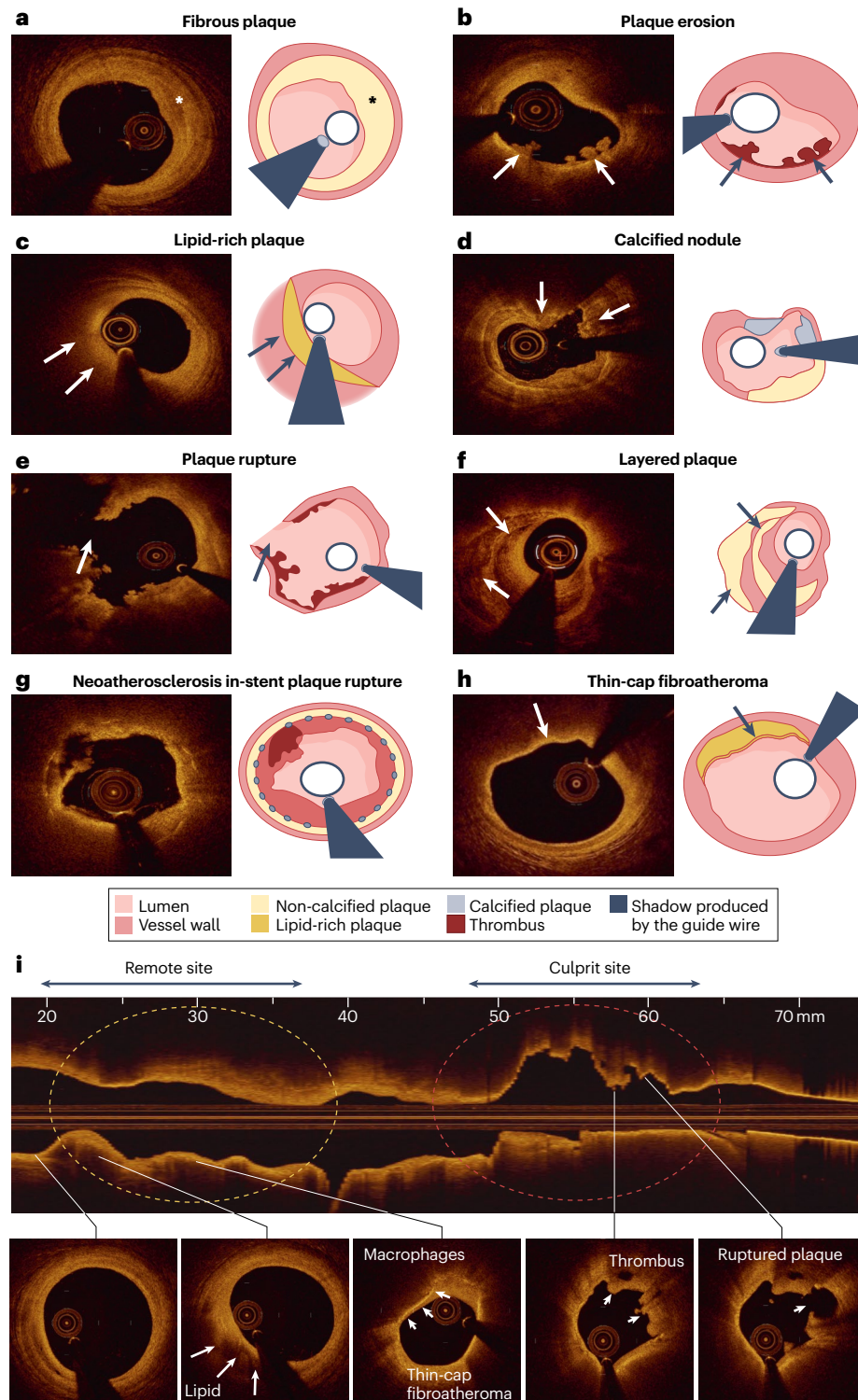


Fig. 10 | OCT for quantitative coronary atherosclerosis imaging. Vulnerable plaque features identified by optical coherence tomography (OCT). The panels on the right of the OCT cross-sectional images are graphic representations of the vessel components. **a**, A fibrous plaque is shown by homogeneous, signal-rich backscattering regions (asterisk). **b**, The presence of attached thrombus (arrows) overlying a visually intact plaque indicates plaque erosion. **c**, A lipid-rich plaque (arrows) can be visualized as low-intensity regions with diffuse borders and high-intensity overlying bands. **d**, One or more regions of calcium protruding into the lumen (arrows) is representative of a calcified nodule. **e**, Plaque rupture (arrow) can be observed as fibrous cap discontinuity and cavity formation within the plaque. **f**, Plaque with layers of different optical densities (arrows) is shown. **g**, The presence of a neoatherosclerosis in-stent plaque rupture is shown by a low-intensity region with diffuse borders and within the stent. **h**, A thin-cap fibroatheroma (arrow) can be visualized as a plaque with lipid-rich content and a fibrous cap <math><65-70 \mu\text{m}</math>. **i**, Longitudinal view and cross-sections below showing different plaque components (lipid-rich plaque, macrophages, thin-cap fibroatheroma, thrombus and ruptured plaque; see arrows in the respective panels) along the left coronary artery. Macrophages are seen as a high-intensity confluent region with a signal intensity exceeding that of background noise (middle panel). Thrombus is seen as a high-intensity backscattering mass protruding into the lumen (middle-right panel).

Consensus statement

a reliable tool to assess stenosis and plaque morphology without exposing the patient to ionizing radiation, provided that further technical improvements can increase the robustness of images. PET has a role in the quantitative assessment of coronary plaque inflammation and is, therefore, the preferred modality for the monitoring and guiding of treatment. ICA is considered the reference standard for the evaluation of patients with stable chest pain and a high probability of coronary stenosis as well as for patients with ACS. IVUS and OCT are intravascular imaging modalities that have a relevant role in the estimation of coronary stenosis severity and in plaque characterization for treatment planning.

The clinical potential of these modalities can be substantially improved by technical advances. For CT, new technologies aimed at improving spatial and temporal resolution as well as at automating the quantification and coronary plaque characterization process will improve its clinical utility. The spatial resolution of MRI can be increased by reducing the voxel size and shortening acquisition times and better signal enhancement can be achieved with new contrast agents. The role of PET will expand with the translation of research findings into clinical practice and the development of new tracers for the detection of plaque vulnerability. Quantitative coronary angiography will help in the standardization of stenotic assessment by ICA, whereas RWS will provide insights into the deformation of the vessel wall caused by coronary plaques. Anatomical measurements by IVUS and OCT will facilitate the determination of coronary flow via the integration of FFR into the same catheters.

No single quantitative coronary imaging modality is optimal for all groups of patients or disease types and not all are equally available with similar local expertise at all clinical centres. Using the Delphi method, we determined which imaging modalities are better suited for specific patient groups (Fig. 3). In conclusion, this clinical Consensus Statement shows the current advantages, disadvantages and expected future development of different imaging modalities for clinical quantitative coronary artery stenosis and atherosclerosis imaging and will help clinicians to choose the most appropriate imaging modality on the basis of the specific clinical scenario, individual patient characteristics and availability of each modality.

Published online: 5 June 2023

References

- Dewey, M. et al. Evaluation of computed tomography in patients with atypical angina or chest pain clinically referred for invasive coronary angiography: randomised controlled trial. *Br. Med. J.* **355**, i5441 (2016).
- Chang, H.-J. et al. Selective referral using CCTA versus direct referral for individuals referred to invasive coronary angiography for suspected CAD: a randomized, controlled, open-label trial. *JACC Cardiovasc. Imaging* **12**, 1303–1312 (2019).
- Rudziński, P. N. et al. Efficacy and safety of coronary computed tomography angiography in patients with a high clinical likelihood of obstructive coronary artery disease. *Kardiol. Pol.* **80**, 56–63 (2022).
- The DISCHARGE Trial Group. CT or invasive coronary angiography in stable chest pain. *N. Engl. J. Med.* **386**, 1591–1602 (2022).
- Kheiri, B. et al. Computed tomography vs invasive coronary angiography in patients with suspected coronary artery disease: a meta-analysis. *JACC Cardiovasc. Imaging* **15**, 2147–2149 (2022).
- Gray, A. J. et al. Early computed tomography coronary angiography in patients with suspected acute coronary syndrome: randomised controlled trial. *Br. Med. J.* **374**, n2106 (2021).
- Schuetz, G. M., Zacharopoulou, N. M., Schlattmann, P. & Dewey, M. Meta-analysis: noninvasive coronary angiography using computed tomography versus magnetic resonance imaging. *Ann. Intern. Med.* **152**, 167–177 (2010).
- Perera, D. et al. Percutaneous revascularization for ischemic left ventricular dysfunction. *N. Engl. J. Med.* **387**, 1351–1360 (2022).
- Fearon, W. F. et al. Fractional flow reserve-guided PCI as compared with coronary bypass surgery. *N. Engl. J. Med.* **386**, 128–137 (2022).
- Stone, G. W. et al. Five-year outcomes after PCI or CABG for left main coronary disease. *N. Engl. J. Med.* **381**, 1820–1830 (2019).
- Velazquez, E. J. et al. Coronary-artery bypass surgery in patients with ischemic cardiomyopathy. *N. Engl. J. Med.* **374**, 1511–1520 (2016).
- Maron, D. J. et al. Initial invasive or conservative strategy for stable coronary disease. *N. Engl. J. Med.* **382**, 1395–1407 (2020).
- Navarese, E. P. et al. Cardiac mortality in patients randomised to elective coronary revascularisation plus medical therapy or medical therapy alone: a systematic review and meta-analysis. *Eur. Heart J.* **42**, 4638–4651 (2021).
- Gaudino, M. et al. Overall and cause-specific mortality in randomized clinical trials comparing percutaneous interventions with coronary bypass surgery: a meta-analysis. *JAMA Intern. Med.* **180**, 1638–1646 (2020).
- Head, S. J. et al. Mortality after coronary artery bypass grafting versus percutaneous coronary intervention with stenting for coronary artery disease: a pooled analysis of individual patient data. *Lancet* **391**, 939–948 (2018).
- Galli, M. et al. Revascularization strategies versus optimal medical therapy in chronic coronary syndrome: a network meta-analysis. *Int. J. Cardiol.* **370**, 58–64 (2023).
- Serruys, P. W. et al. Percutaneous coronary intervention versus coronary-artery bypass grafting for severe coronary artery disease. *N. Engl. J. Med.* **360**, 961–972 (2009).
- Farooq, V. et al. Anatomical and clinical characteristics to guide decision making between coronary artery bypass surgery and percutaneous coronary intervention for individual patients: development and validation of SYNTAX score II. *Lancet* **381**, 639–650 (2013).
- Takahashi, K. et al. Redevelopment and validation of the SYNTAX score II to individualise decision making between percutaneous and surgical revascularisation in patients with complex coronary artery disease: secondary analysis of the multicentre randomised controlled SYNTAXES trial with external cohort validation. *Lancet* **396**, 1399–1412 (2020).
- Hara, H. et al. External validation of the SYNTAX Score II 2020. *J. Am. Coll. Cardiol.* **78**, 1227–1238 (2021).
- Doenst, T. et al. PCI and CABG for treating stable coronary artery disease. *J. Am. Coll. Cardiol.* **73**, 964–976 (2019).
- Stone, P. H., Libby, P. & Boden, W. E. Fundamental pathobiology of coronary atherosclerosis and clinical implications for chronic ischemic heart disease management — the plaque hypothesis: a narrative review. *JAMA Cardiol.* <https://doi.org/10.1001/jamacardio.2022.3926> (2022).
- Ferraro, R. et al. Evaluation and management of patients with stable angina: beyond the ischemia paradigm. *J. Am. Coll. Cardiol.* **76**, 2252–2266 (2020).
- Ali, Z. et al. Optical coherence tomography-guided coronary stent implantation compared to angiography: a multicentre randomised trial in PCI — design and rationale of ILLUMIEN IV: OPTIMAL PCI. *EuroIntervention* **16**, 1092–1099 (2021).
- Stone, G. W. et al. A prospective natural-history study of coronary atherosclerosis. *N. Engl. J. Med.* **364**, 226–235 (2011).
- Hajhosseiny, R. et al. Coronary magnetic resonance angiography: technical innovations leading us to the promised land? *JACC Cardiovasc. Imaging* **13**, 2653–2672 (2020).
- Joshi, N. V. et al. ¹⁸F-fluoride positron emission tomography for identification of ruptured and high-risk coronary atherosclerotic plaques: a prospective clinical trial. *Lancet* **383**, 705–713 (2014).
- Garcia, S. et al. Outcomes after complete versus incomplete revascularization of patients with multivessel coronary artery disease: a meta-analysis of 89,883 patients enrolled in randomized clinical trials and observational studies. *J. Am. Coll. Cardiol.* **62**, 1421–1431 (2013).
- Dweck, M. R. et al. Imaging of coronary atherosclerosis — evolution towards new treatment strategies. *Nat. Rev. Cardiol.* **13**, 533–548 (2016).
- Andreini, D. et al. Pre-procedural planning of coronary revascularization by cardiac computed tomography: an expert consensus document of the Society of Cardiovascular Computed Tomography. *EuroIntervention* **18**, e872–e887 (2022).
- Xiong, T.-Y. et al. Transcatheter aortic valve implantation in patients with bicuspid valve morphology: a roadmap towards standardization. *Nat. Rev. Cardiol.* **20**, 52–67 (2023).
- Gorog, D. A. et al. Current and novel biomarkers of thrombotic risk in COVID-19: a Consensus Statement from the International COVID-19 Thrombosis Biomarkers Colloquium. *Nat. Rev. Cardiol.* **19**, 475–495 (2022).
- Alvarenga, A. et al. Scenarios for population health inequalities in 2030 in Europe: the EURO-HEALTHY project experience. *Int. J. Equity Health* **18**, 100 (2019).
- Veeranki, S. P. et al. A Delphi consensus approach for difficult-to-treat patients with severe hemophilia A without inhibitors. *J. Blood Med.* **12**, 913–928 (2021).
- Dewey, M. et al. Clinical quantitative cardiac imaging for the assessment of myocardial ischaemia. *Nat. Rev. Cardiol.* **17**, 427–450 (2020).
- Budoff, M. J. et al. Cardiac CT angiography in current practice: an American Society for preventive cardiology clinical practice statement. *Am. J. Prev. Cardiol.* **9**, 100318 (2022).
- Wong, N. D. et al. Atherosclerotic cardiovascular disease risk assessment: an American Society for Preventive Cardiology clinical practice statement. *Am. J. Prev. Cardiol.* **10**, 100335 (2022).
- Halliburton, S. et al. State-of-the-art in CT hardware and scan modes for cardiovascular CT. *J. Cardiovasc. Comput. Tomogr.* **6**, 154–163 (2012).
- Song, Y. B. et al. Contemporary discrepancies of stenosis assessment by computed tomography and invasive coronary angiography. *Circ. Cardiovasc. Imaging* **12**, e007720 (2019).
- Krazinski, A. W. et al. Reduced radiation dose and improved image quality at cardiovascular CT angiography by automated attenuation-based tube voltage selection: intra-individual comparison. *Eur. Radiol.* **24**, 2677–2684 (2014).

Consensus statement

41. Dweck, M. R., Puntman, V., Vesey, A. T., Fayad, Z. A. & Nagel, E. MR imaging of coronary arteries and plaques. *JACC Cardiovasc. Imaging* **9**, 306–316 (2016).
42. Schönerberger, E. et al. Kidney injury after intravenous versus intra-arterial contrast agent in patients suspected of having coronary artery disease: a randomized trial. *Radiology* **292**, 664–672 (2019).
43. Bosserd, M. et al. Serum creatinine baseline fluctuation and acute kidney injury after intravenous or intra-arterial contrast agent administration—an intraindividual comparison as part of a randomized controlled trial. *Nephrol. Dial. Transplant.* **37**, 1191–1194 (2022).
44. Bustin, A. et al. Five-minute whole-heart coronary MRA with sub-millimeter isotropic resolution, 100% respiratory scan efficiency, and 3D-PROST reconstruction. *Magn. Reson. Med.* **81**, 102–115 (2019).
45. Kato, Y. et al. Non-contrast coronary magnetic resonance angiography: current frontiers and future horizons. *Magma* **33**, 591–612 (2020).
46. Nagata, M. et al. Diagnostic accuracy of 1.5-T unenhanced whole-heart coronary MR angiography performed with 32-channel cardiac coils: initial single-center experience. *Radiology* **259**, 384–392 (2011).
47. Makowski, M. R. et al. Characterization of coronary atherosclerosis by magnetic resonance imaging. *Circulation* **128**, 1244–1255 (2013).
48. Jansen, C. H. P. et al. Detection of intracoronary thrombus by magnetic resonance imaging in patients with acute myocardial infarction. *Circulation* **124**, 416–424 (2011).
49. Ehara, S. et al. Hyperintense plaque identified by magnetic resonance imaging relates to intracoronary thrombus as detected by optical coherence tomography in patients with angina pectoris. *Eur. Heart J. Cardiovasc. Imaging* **13**, 394–399 (2012).
50. Tarkin, J. M. et al. Imaging atherosclerosis. *Circ. Res.* **118**, 750–769 (2016).
51. Dewey, M., Schink, T. & Dewey, C. F. Frequency of referral of patients with safety-related contraindications to magnetic resonance imaging. *Eur. J. Radiol.* **63**, 124–127 (2007).
52. Hucker, W. J. & Jaffer, F. A. F-FDG PET imaging of atherosclerosis—a new approach to detect inflamed, high-risk coronary plaques? *Curr. Cardiovasc. Imaging Rep.* **4**, 1–3 (2011).
53. Sun, Z.-H., Rashmizal, H. & Xu, L. Molecular imaging of plaques in coronary arteries with PET and SPECT. *J. Geriatr. Cardiol.* **11**, 259–273 (2014).
54. Kennedy-Dixon, T.-G., Gossell-Williams, M., Cooper, M., Trabalsi, M. & Vinjamuri, S. Evaluation of Radiopharmaceutical adverse reaction reports to the British Nuclear Medicine Society from 2007 to 2016. *J. Nucl. Med.* **58**, 2010–2012 (2017).
55. Silberstein, E. B. Prevalence of adverse events to radiopharmaceuticals from 2007 to 2011. *J. Nucl. Med.* **55**, 1308–1310 (2014).
56. Mayer, M. et al. Imaging atherosclerosis by PET, with emphasis on the role of FDG and NaF as potential biomarkers for this disorder. *Front. Physiol.* **11**, 511391 (2020).
57. Leccisotti, L., Nicoletti, P., Cappiello, C., Indovina, L. & Giordano, A. PET imaging of vulnerable coronary artery plaques. *Clin. Transl. Imaging* **7**, 267–284 (2019).
58. Verberne, H. J. et al. EANM procedural guidelines for radionuclide myocardial perfusion imaging with SPECT and SPECT/CT: 2015 revision. *Eur. J. Nucl. Med. Mol. Imaging* **42**, 1929–1940 (2015).
59. Green, N. E. et al. Angiographic views used for percutaneous coronary interventions: a three-dimensional analysis of physician-determined vs. computer-generated views. *Catheter. Cardiovasc. Interv.* **64**, 451–459 (2005).
60. Brugaletta, S. et al. NIRS and IVUS for characterization of atherosclerosis in patients undergoing coronary angiography. *JACC Cardiovasc. Imaging* **4**, 647–655 (2011).
61. Saito, Y. et al. Clinical expert consensus document on standards for measurements and assessment of intravascular ultrasound from the Japanese Association of Cardiovascular Intervention and Therapeutics. *Cardiovasc. Interv. Ther.* **35**, 1–12 (2020).
62. Akasaka, T. et al. Pathophysiology of acute coronary syndrome assessed by optical coherence tomography. *J. Cardiol.* **56**, 8–14 (2010).
63. Araki, M. et al. Optical coherence tomography in coronary atherosclerosis assessment and intervention. *Nat. Rev. Cardiol.* **19**, 684–703 (2022).
64. Johnson, T. W. et al. Clinical use of intracoronary imaging. Part 2: acute coronary syndromes, ambiguous coronary angiography findings, and guiding interventional decision-making: an expert consensus document of the European Association of Percutaneous Cardiovascular Interventions. *Eur. Heart J.* **40**, 2566–2584 (2019).
65. Mintz, G. S. & Guagliumi, G. Intravascular imaging in coronary artery disease. *Lancet* **390**, 793–809 (2017).
66. Hausmann, D. et al. The safety of intracoronary ultrasound. A multicenter survey of 2207 examinations. *Circulation* **91**, 623–630 (1995).
67. Dewey, M. et al. Noninvasive coronary angiography by 320-row computed tomography with lower radiation exposure and maintained diagnostic accuracy: comparison of results with cardiac catheterization in a head-to-head pilot investigation. *Circulation* **120**, 867–875 (2009).
68. von Ballmoos, M. W., Haring, B., Juillerat, P. & Alkadhi, H. Meta-analysis: diagnostic performance of low-radiation-dose coronary computed tomography angiography. *Ann. Intern. Med.* **154**, 413–420 (2011).
69. Haase, R. et al. Diagnosis of obstructive coronary artery disease using computed tomography angiography in patients with stable chest pain depending on clinical probability and in clinically important subgroups: meta-analysis of individual patient data. *Br. Med. J.* **365**, 11945 (2019).
70. Kim, W. Y. et al. Coronary magnetic resonance angiography for the detection of coronary stenoses. *N. Engl. J. Med.* **345**, 1863–1869 (2001).
71. Kato, S. et al. Assessment of coronary artery disease using magnetic resonance coronary angiography: a national multicenter trial. *J. Am. Coll. Cardiol.* **56**, 983–991 (2010).
72. Figtree, G. A. et al. Noninvasive plaque imaging to accelerate coronary artery disease drug development. *Circulation* **146**, 1712–1727 (2022).
73. Tonino, P. A. L. et al. Angiographic versus functional severity of coronary artery stenoses in the FAME study fractional flow reserve versus angiography in multivessel evaluation. *J. Am. Coll. Cardiol.* **55**, 2816–2821 (2010).
74. Koo, B.-K. et al. Fractional flow reserve or intravascular ultrasonography to guide PCI. *N. Engl. J. Med.* **387**, 779–789 (2022).
75. Mintz, G. S., Matsumura, M., Ali, Z. & Maehara, A. Clinical utility of intravascular imaging: past, present, and future. *JACC Cardiovasc. Imaging* **15**, 1799–1820 (2022).
76. Arbab-Zadeh, A. & Hoe, J. Quantification of coronary arterial stenoses by multidetector CT angiography in comparison with conventional angiography methods, caveats, and implications. *JACC Cardiovasc. Imaging* **4**, 191–202 (2011).
77. Zir, L. M., Miller, S. W., Dinsmore, R. E., Gilbert, J. P. & Harthorne, J. W. Interobserver variability in coronary angiography. *Circulation* **53**, 627–632 (1976).
78. Nallamothu, B. K. et al. Comparison of clinical interpretation with visual assessment and quantitative coronary angiography in patients undergoing percutaneous coronary intervention in contemporary practice: the Assessing Angiography (A2) project. *Circulation* **127**, 1793–1800 (2013).
79. Kubo, T. et al. OCT compared with IVUS in a coronary lesion assessment: the OPUS-CLASS study. *JACC Cardiovasc. Imaging* **6**, 1095–1104 (2013).
80. Nishi, T. et al. Head-to-head comparison of quantitative measurements between intravascular imaging systems: an in vitro phantom study. *Int. J. Cardiol.* **36**, 100867 (2021).
81. Douglas, P. S. et al. Outcomes of anatomical versus functional testing for coronary artery disease. *N. Engl. J. Med.* **372**, 1291–1300 (2015).
82. SCOT-HEART investigators CT coronary angiography in patients with suspected angina due to coronary heart disease (SCOT-HEART): an open-label, parallel-group, multicentre trial. *Lancet* **385**, 2383–2391 (2015).
83. Hajhosseini, R. et al. Clinical comparison of sub-mm high-resolution non-contrast coronary CMR angiography against coronary CT angiography in patients with low-intermediate risk of coronary artery disease: a single center trial. *J. Cardiovasc. Magn. Reson.* **23**, 57 (2021).
84. Park, S.-J. et al. Intravascular ultrasound-derived minimal lumen area criteria for functionally significant left main coronary artery stenosis. *JACC Cardiovasc. Interv.* **7**, 868–874 (2014).
85. D’Ascenzo, F. et al. Accuracy of intravascular ultrasound and optical coherence tomography in identifying functionally significant coronary stenosis according to vessel diameter: a meta-analysis of 2,581 patients and 2,807 lesions. *Am. Heart J.* **169**, 663–673 (2015).
86. Mergen, V. et al. Ultra-high-resolution coronary CT angiography with photon-counting detector CT: feasibility and image characterization. *Investig. Radiol.* **57**, 780–788 (2022).
87. Boccalini, S. et al. First in-human results of computed tomography angiography for coronary stent assessment with a spectral photon counting computed tomography. *Investig. Radiol.* **57**, 212–221 (2022).
88. Küstner, T. et al. Deep-learning based super-resolution for 3D isotropic coronary MR angiography in less than a minute. *Magn. Reson. Med.* **86**, 2837–2852 (2021).
89. Yu, W. et al. Diagnostic accuracy of intracoronary optical coherence tomography-derived fractional flow reserve for assessment of coronary stenosis severity. *EuroIntervention* **15**, 189–197 (2019).
90. Yu, W. et al. Accuracy of intravascular ultrasound-based fractional flow reserve in identifying hemodynamic significance of coronary stenosis. *Circ. Cardiovasc. Interv.* **14**, e009840 (2021).
91. Kolossváry, M., Szilveszter, B., Merkely, B. & Maurovich-Horvat, P. Plaque imaging with CT—a comprehensive review on coronary CT angiography based risk assessment. *Cardiovasc. Diagn. Ther.* **7**, 489–506 (2017).
92. Motwani, M. High-risk plaque features on coronary computed tomography angiography: a long-term relationship: it’s complicated! *Eur. Heart J. Cardiovasc. Imaging* **21**, 249–250 (2019).
93. Rumberger, J. A. & Kaufman, L. A rosetta stone for coronary calcium risk stratification: agatston, volume, and mass scores in 11,490 individuals. *Am. J. Roentgenol.* **181**, 743–748 (2003).
94. Latif, M. A., Budoff, M. J. & Greenland, P. *Cardiac CT 2 edn* (Springer Berlin Heidelberg, 2014).
95. Budoff, M. J. et al. Ten-year association of coronary artery calcium with atherosclerotic cardiovascular disease (ASCVD) events: the Multi-Ethnic Study of Atherosclerosis (MESA). *Eur. Heart J.* **39**, 2401–2408 (2018).
96. Hollenberg, E. J. et al. Relationship between coronary artery calcium and atherosclerosis progression among patients with suspected coronary artery disease. *JACC Cardiovasc. Imaging* **15**, 1063–1074 (2022).
97. Grundy, S. M. et al. AHA/ACC/AACVPR/AAPA/ABC/ACPM/ADA/AGS/APHA/ASPC/NLA/PCNA guideline on the management of blood cholesterol: executive summary: a report of the American College of Cardiology/American Heart Association Task Force on Clinical Practice Guidelines. *Circulation* **139**, e1046–e1081 (2019).
98. Williams, M. C. et al. Low-attenuation noncalcified plaque on coronary computed tomography angiography predicts myocardial infarction: results from the multicenter SCOT-HEART trial (Scottish Computed Tomography of the HEART). *Circulation* **141**, 1452–1462 (2020).
99. Dweck, M. R. et al. Contemporary rationale for non-invasive imaging of adverse coronary plaque features to identify the vulnerable patient: a Position Paper from the European Society of Cardiology Working Group on Atherosclerosis and Vascular Biology and the European Association of Cardiovascular Imaging. *Eur. Heart J. Cardiovasc. Imaging* **21**, 1177–1183 (2020).

100. Greenland, P. & Lloyd-Jones, D. M. Role of coronary artery calcium testing for risk assessment in primary prevention of atherosclerotic cardiovascular disease: a review. *JAMA Cardiol.* **7**, 219–224 (2022).
101. Tzolos, E. et al. Pericoronary adipose tissue attenuation, low-attenuation plaque burden, and 5-year risk of myocardial infarction. *JACC Cardiovasc. Imaging* **15**, 1078–1088 (2022).
102. Feger, S. et al. Effect of computed tomography versus invasive coronary angiography on statin adherence: a randomized controlled trial. *JACC Cardiovasc. Imaging* **14**, 1480–1483 (2021).
103. Antonopoulos, A. S. et al. Detecting human coronary inflammation by imaging perivascular fat. *Sci. Transl. Med.* **9**, eaal2658 (2017).
104. Sermesant, M., Delingette, H., Cochet, H., Jais, P. & Ayache, N. Applications of artificial intelligence in cardiovascular imaging. *Nat. Rev. Cardiol.* **18**, 600–609 (2021).
105. Elnabawi, Y. A. et al. Association of biologic therapy with coronary inflammation in patients with psoriasis as assessed by perivascular fat attenuation index. *JAMA Cardiol.* **4**, 885–891 (2019).
106. Oikonomou, E. K. et al. Non-invasive detection of coronary inflammation using computed tomography and prediction of residual cardiovascular risk (the CRISP CT study): a post-hoc analysis of prospective outcome data. *Lancet* **392**, 929–939 (2018).
107. Botnar, R. M. et al. Noninvasive coronary vessel wall and plaque imaging with magnetic resonance imaging. *Circulation* **102**, 2582–2587 (2000).
108. Kim, W. Y. et al. Three-dimensional black-blood cardiac magnetic resonance coronary vessel wall imaging detects positive arterial remodeling in patients with nonsignificant coronary artery disease. *Circulation* **106**, 296–299 (2002).
109. Hays, A. G. et al. Local coronary wall eccentricity and endothelial function are closely related in patients with atherosclerotic coronary artery disease. *J. Cardiovasc. Magn. Reson.* **19**, 51 (2017).
110. Miao, C. et al. Positive remodeling of the coronary arteries detected by magnetic resonance imaging in an asymptomatic population: MESA (Multi-Ethnic Study of Atherosclerosis). *J. Am. Coll. Cardiol.* **53**, 1708–1715 (2009).
111. Gerretsen, S. et al. Detection of coronary plaques using MR coronary vessel wall imaging: validation of findings with intravascular ultrasound. *Eur. Radiol.* **23**, 115–124 (2013).
112. Noguchi, T. et al. High-intensity signals in coronary plaques on noncontrast T1-weighted magnetic resonance imaging as a novel determinant of coronary events. *J. Am. Coll. Cardiol.* **63**, 989–999 (2014).
113. Yeon, S. B. et al. Delayed-enhancement cardiovascular magnetic resonance coronary artery wall imaging: comparison with multislice computed tomography and quantitative coronary angiography. *J. Am. Coll. Cardiol.* **50**, 441–447 (2007).
114. Kawasaki, T. et al. Characterization of hyperintense plaque with noncontrast T₁-weighted cardiac magnetic resonance coronary plaque imaging: comparison with multislice computed tomography and intravascular ultrasound. *JACC Cardiovasc. Imaging* **2**, 720–728 (2009).
115. Noguchi, T. et al. Effect of intensive statin therapy on coronary high-intensity plaques detected by noncontrast T1-weighted imaging: the AQUAMARINE pilot study. *J. Am. Coll. Cardiol.* **66**, 245–256 (2015).
116. Sato, S. et al. Coronary high-intensity plaques at T1-weighted MRI in stable coronary artery disease: comparison with near-infrared spectroscopy intravascular US. *Radiology* **302**, 557–565 (2022).
117. Dewey, M. Coronary CT versus MR angiography: pro CT — the role of CT angiography. *Radiology* **258**, 329–339 (2011).
118. Mulder, W. J. M. et al. Magnetic resonance molecular imaging contrast agents and their application in atherosclerosis. *Top. Magn. Reson. Imaging* **18**, 409–417 (2007).
119. Dargot, E. et al. Towards quantification of inflammation in atherosclerotic plaque in the clinic — characterization and optimization of fluorine-19 MRI in mice at 3T. *Sci. Rep.* **9**, 17488 (2019).
120. Nazir, M. S. et al. High-resolution non-contrast free-breathing coronary cardiovascular magnetic resonance angiography for detection of coronary artery disease: validation against invasive coronary angiography. *J. Cardiovasc. Magn. Reson.* **24**, 26 (2022).
121. Tawakol, A. et al. Relation between resting amygdalar activity and cardiovascular events: a longitudinal and cohort study. *Lancet* **389**, 834–845 (2017).
122. Cheng, V. Y. et al. Coronary arterial ¹⁸F-FDG uptake by fusion of PET and coronary CT angiography at sites of percutaneous stenting for acute myocardial infarction and stable coronary artery disease. *J. Nucl. Med.* **53**, 575–583 (2012).
123. Borchert, T. et al. Dissecting the target leukocyte subpopulations of clinically relevant inflammation radiopharmaceuticals. *J. Nucl. Cardiol.* **28**, 1636–1645 (2021).
124. Tarkin, J. M. et al. Detection of atherosclerotic inflammation by ⁶⁸Ga-DOTATATE PET compared to [¹⁸F]FDG PET imaging. *J. Am. Coll. Cardiol.* **69**, 1774–1791 (2017).
125. Kwiecinski, J. et al. Coronary ¹⁸F-sodium fluoride uptake predicts outcomes in patients with coronary artery disease. *J. Am. Coll. Cardiol.* **75**, 3061–3074 (2020).
126. Ishiwata, Y. et al. Quantification of temporal changes in calcium score in active atherosclerotic plaque in major vessels by ¹⁸F-sodium fluoride PET/CT. *Eur. J. Nucl. Med. Mol. Imaging* **44**, 1529–1537 (2017).
127. Fayad, Z. A. et al. Safety and efficacy of dalcetrapib on atherosclerotic disease using novel non-invasive multimodality imaging (dal-PLAQUE): a randomised clinical trial. *Lancet* **378**, 1547–1559 (2011).
128. Vucic, E. et al. Regression of inflammation in atherosclerosis by the LXR agonist R211945: a noninvasive assessment and comparison with atorvastatin. *JACC Cardiovasc. Imaging* **5**, 819–828 (2012).
129. van der Valk, F. M. et al. Increased haematopoietic activity in patients with atherosclerosis. *Eur. Heart J.* **38**, 425–432 (2017).
130. US National Library of Medicine. *ClinicalTrials.gov* <https://clinicaltrials.gov/ct2/show/NCT02278211> (2015).
131. Wu, M. et al. Feasibility of in vivo imaging of fibroblast activation protein in human arterial walls. *J. Nucl. Med.* **63**, 948–951 (2022).
132. Tzolos, E. et al. Noninvasive in vivo coronary artery thrombus imaging. *JACC Cardiovasc. Imaging* <https://doi.org/10.1016/j.jcmg.2022.10.002> (2022).
133. Derlin, T. et al. Exploring vessel wall biology in vivo by ultra-sensitive total-body positron emission tomography. *J. Nucl. Med.* <https://doi.org/10.2967/jnumed.122.264550> (2022).
134. Derlin, T. et al. Imaging of chemokine receptor CXCR4 expression in culprit and nonculprit coronary atherosclerotic plaque using motion-corrected [⁶⁸Ga]pentixafor PET/CT. *Eur. J. Nucl. Med. Mol. Imaging* **45**, 1934–1944 (2018).
135. Hong, H. et al. Radial wall strain: a novel angiographic measure of plaque composition and vulnerability. *EuroIntervention* <https://doi.org/10.4244/EIJ-D-22-00537> (2022).
136. Neumann, F.-J. et al. ESC/EACTS guidelines on myocardial revascularization. *Eur. Heart J.* **40**, 87–165 (2019).
137. Huang, D. et al. Assessment of endothelial shear stress in patients with mild or intermediate coronary stenoses using coronary computed tomography angiography: comparison with invasive coronary angiography. *Int. J. Cardiovasc. Imaging* **33**, 1101–1110 (2017).
138. Kröner, E. S. J. et al. Positive remodeling on coronary computed tomography as a marker for plaque vulnerability on virtual histology intravascular ultrasound. *Am. J. Cardiol.* **107**, 1725–1729 (2011).
139. Waksman, R. et al. Identification of patients and plaques vulnerable to future coronary events with near-infrared spectroscopy intravascular ultrasound imaging: a prospective, cohort study. *Lancet* **394**, 1629–1637 (2019).
140. Xu, J. & Lo, S. Fundamentals and role of intravascular ultrasound in percutaneous coronary intervention. *Cardiovasc. Diagn. Ther.* **10**, 1358–1370 (2020).
141. Zhang, J. et al. Intravascular ultrasound versus angiography-guided drug-eluting stent implantation: the ULTIMATE trial. *J. Am. Coll. Cardiol.* **72**, 3126–3137 (2018).
142. Volleberg, R. et al. Optical coherence tomography and coronary revascularization: from indication to procedural optimization. *Trends Cardiovasc. Med.* **33**, 92–106 (2021).
143. Jodas, D. S., Pereira, A. S. & Tavares, J. M. R. S. Automatic segmentation of the lumen region in intravascular images of the coronary artery. *Med. Image Anal.* **40**, 60–79 (2017).
144. Souteyrand, G. et al. Mechanisms of stent thrombosis analysed by optical coherence tomography: insights from the national PESTO French registry. *Eur. Heart J.* **37**, 1208–1216 (2016).
145. Joner, M. et al. Neoatherosclerosis in patients with coronary stent thrombosis: findings from optical coherence tomography imaging (a report of the PRESTIGE Consortium). *JACC Cardiovasc. Interv.* **11**, 1340–1350 (2018).
146. Adriaenssens, T. et al. Optical coherence tomography findings in patients with coronary stent thrombosis: a report of the PRESTIGE consortium (Prevention of Late Stent Thrombosis by an Interdisciplinary Global European Effort). *Circulation* **136**, 1007–1021 (2017).
147. Shimokado, A. et al. In vivo optical coherence tomography imaging and histopathology of healed coronary plaques. *Atherosclerosis* **275**, 35–42 (2018).
148. Akl, E. et al. First in-human evaluation of a novel intravascular ultrasound and optical coherence tomography system for intracoronary imaging. *Catheter. Cardiovasc. Interv.* **99**, 686–698 (2022).
149. Araki, M. et al. Predictors of rapid plaque progression: an optical coherence tomography study. *JACC Cardiovasc. Imaging* **14**, 1628–1638 (2021).
150. Ali, Z. A. et al. Optical coherence tomography compared with intravascular ultrasound and with angiography to guide coronary stent implantation (ILUMIEN III: OPTIMIZE PCI): a randomised controlled trial. *Lancet* **388**, 2618–2628 (2016).
151. Chu, M. et al. Artificial intelligence and optical coherence tomography for the automatic characterisation of human atherosclerotic plaques. *EuroIntervention* **17**, 41–50 (2021).
152. Hebsgaard, L. et al. Co-registration of optical coherence tomography and X-ray angiography in percutaneous coronary intervention: the does optical coherence tomography optimize revascularization (DOCTOR) fusion study. *Int. J. Cardiol.* **182**, 272–278 (2015).
153. Gardner, C. M. et al. Detection of lipid core coronary plaques in autopsy specimens with a novel catheter-based near-infrared spectroscopy system. *JACC Cardiovasc. Imaging* **1**, 638–648 (2008).
154. Kakizaki, S. et al. Optical coherence tomography fractional flow reserve and cardiovascular outcomes in patients with acute coronary syndrome. *JACC Cardiovasc. Interv.* **15**, 2035–2048 (2022).
155. Gosling, O. et al. A comparison of radiation doses between state-of-the-art multislice CT coronary angiography with iterative reconstruction, multislice CT coronary angiography with standard filtered back-projection and invasive diagnostic coronary angiography. *Heart* **96**, 922–926 (2010).
156. Herzog, B. A. et al. First head-to-head comparison of effective radiation dose from low-dose 64-slice CT with prospective ECG-triggering versus invasive coronary angiography. *Heart* **95**, 1656–1661 (2009).
157. Dorbala, S. et al. SNMMI/ASNC/SCCT guideline for cardiac SPECT/CT and PET/CT 1.0. *J. Nucl. Med.* **54**, 1485–1507 (2013).
158. Beheshti, M. et al. ¹⁸F-NaF PET/CT: EANM procedure guidelines for bone imaging. *Eur. J. Nucl. Med. Mol. Imaging* **42**, 1767–1777 (2015).
159. van der Sijde, J. N. et al. Safety of optical coherence tomography in daily practice: a comparison with intravascular ultrasound. *Eur. Heart J. Cardiovasc. Imaging* **18**, 467–474 (2017).

Consensus statement

160. Stuber, M., Börner, P., Spuentrup, E., Botnar, R. M. & Manning, W. J. Selective three-dimensional visualization of the coronary arterial lumen using arterial spin tagging. *Magn. Reson. Med.* **47**, 322–329 (2002).
161. Stuber, M., Botnar, R. M., Spuentrup, E., Kissinger, K. V. & Manning, W. J. Three-dimensional high-resolution fast spin-echo coronary magnetic resonance angiography. *Magn. Reson. Med.* **45**, 206–211 (2001).

Acknowledgements

We thank the German Research Foundation (DFG) for funding the Second Quantitative Cardiovascular Imaging Meeting and this Consensus Statement on the quantitative assessment of coronary artery stenosis and atherosclerosis (DE 1361/22-1). This work was also supported by the DFG through its graduate programme on quantitative biomedical imaging (BIOQIC, GRK 2260/1, DFG project number: 289347353), the DFG Priority Programme Radiomics (DFG project number: 402688427) for the investigation of coronary plaque and coronary flow (DE 1361/19-1: DFG project number: 428222922 and DE 1361/20-1: DFG project number: 428223139 in SPP 2177/1), and the GUIDE-IT project on data sharing of medical imaging trials (DE 1361/24-1, DFG project number: 495697118).

Author contributions

The authors contributed substantially to all aspects of the article.

Competing interests

V.F. has received educational grants, fees for lectures and speeches, fees for professional consultation, and research and study funds from Abbott, Abiomed, Berlin Heart, Biotronik, Boston Scientific, CryoLife, Edwards Lifesciences, LivaNova, Medtronic, Novartis and Zurich Heart. H.A. has received institutional grants from Bayer, Canon, Guerbet and Siemens, and is currently part of the speaker's bureau for Siemens. I.I. has received institutional research grants from Esaote and Pie Medical Imaging. She has also received an institutional research grant funded by the Dutch Technology Foundation together with Pie Medical Imaging BV and Philips Healthcare and is co-inventor on patents (US 10,176,575 B2; US 10,395,366 B2; US 11,004,198 B2; US 10,699,407 B2) and patent applications (17317746, 16911323) on the detection of functionally significant coronary stenosis. P.M.-H. is a shareholder of Neumann Medical. K.M.C. is a co-founder and shareholder in Caristo Diagnostics, a University of Oxford spin-out company involved in medical imaging. R.M. has received speaker fees from Bayer and Siemens. M.S. has received non-monetary research support from Siemens Healthineers. A.C.'s spouse is employed by GE Healthcare. D.D. has received software royalties from

Cedars-Sinai Medical Center. F.G.M. has received a research grant from GE Healthcare and speaker honoraria from Bayer Vital, Circle Cardiovascular Imaging and GE Healthcare. M.R.D. has received speaker fees from Edwards, Novartis and Pfizer, and has received consultancy fees from Beren, Jupiter Bioventures, Novartis and Silence Therapeutics. J.J.P. is a consultant for Philips. U.L. has received research grants to institutions from Abbott and is an honorary advisory lecturer for Abbott and Boston Scientific. G.G. has a consultant agreement with Abbott Vascular, Gentuity, Infraredx and Panovision, and has received a research grant from Abbott Vascular, Amgen and Infraredx. A.A.G. reports speaker honoraria from GE Healthcare. M.C.W. has given talks for Canon Medical Systems, Novartis and Siemens Healthineers. D.E.N. has received grants, acts as a consultant and has clinical trial contracts with Abbott, Amgen, AstraZeneca, Autoplaque, BMS, Boehringer Ingelheim, Eli Lilly, GE Healthcare, GSK, Janssen, Life Molecular Imaging, MSD, Novartis, Pfizer, Phillips, Roche, Sanofi, Siemens, Silence Technologies, SOFIE, Toshiba, UCB, Vifor, Wyeth and Zealand. M.D. is the editor of *Cardiac CT* (published by Springer Nature) and offers hands-on courses on CT imaging (www.ct-kurs.de), and has institutional research agreements with Canon, General Electric, Philips and Siemens. The terms of these arrangements are managed by the legal department of Charité – Universitätsmedizin Berlin. He also holds a joint approved patent with Florian Michallek on fractal analysis of medical imaging (EPO 2022 EP3350773A1 and USPTO 2021 10,991,109). The other authors declare no competing interests.

Additional information

Supplementary information The online version contains supplementary material available at <https://doi.org/10.1038/s41569-023-00880-4>.

Peer review information *Nature Reviews Cardiology* thanks Matthew Budoff and the other, anonymous, reviewer(s) for their contribution to the peer review of this work.

Publisher's note Springer Nature remains neutral with regard to jurisdictional claims in published maps and institutional affiliations.

Springer Nature or its licensor (e.g. a society or other partner) holds exclusive rights to this article under a publishing agreement with the author(s) or other rightsholder(s); author self-archiving of the accepted manuscript version of this article is solely governed by the terms of such publishing agreement and applicable law.

© Springer Nature Limited 2023

Aldo J. Vázquez Mézquita^{1,2,8}, **Federico Bivati**^{1,2,8}, **Volkmar Falk**^{2,3,4}, **Hatem Alkadhi**⁵, **Reza Hajhosseiny**^{6,7}, **Pál Maurovich-Horvat**⁸, **Robert Manka**^{5,9}, **Sebastian Kozerke**¹⁰, **Matthias Stuber**¹¹, **Thorsten Derlin**¹², **Keith M. Channon**¹³, **Ivana Išgum**¹⁴, **Adriaan Coenen**¹⁵, **Bernhard Foellmer**¹, **Damini Dey**¹⁶, **Rick H. J. A. Volleberg**¹⁷, **Felix G. Meinel**¹⁸, **Marc R. Dweck**¹⁹, **Jan J. Piek**²⁰, **Tim van de Hoef**²¹, **Ulf Landmesser**^{3,22}, **Giulio Guagliumi**²³, **Andreas A. Giannopoulos**²⁴, **René M. Botnar**^{6,25}, **Ramzi Khamis**⁷, **Michelle C. Williams**¹⁹, **David E. Newby**^{19,29} & **Marc Dewey**^{1,3,26,27,29} ✉

¹Department of Radiology, Charité – Universitätsmedizin Berlin, Berlin, Germany. ²Department of Cardiothoracic and Vascular Surgery, Deutsches Herzzentrum der Charité (DHZC), Charité – Universitätsmedizin Berlin, Berlin, Germany. ³DZHK (German Centre for Cardiovascular Research) Partner Site, Berlin, Germany. ⁴Department of Health Science and Technology, ETH Zurich, Zurich, Switzerland. ⁵Diagnostic and Interventional Radiology, University Hospital Zurich, University of Zurich, Zurich, Switzerland. ⁶School of Biomedical Engineering and Imaging Sciences, King's College London, London, UK. ⁷National Heart and Lung Institute, Imperial College London, London, UK. ⁸Department of Radiology, Medical Imaging Center, Semmelweis University, Budapest, Hungary. ⁹Department of Cardiology, University Heart Center, University Hospital Zurich, Zurich, Switzerland. ¹⁰Institute for Biomedical Engineering, ETH Zurich, University of Zurich, Zurich, Switzerland. ¹¹Department of Radiology, Centre Hospitalier Universitaire Vaudois, Lausanne, Switzerland. ¹²Department of Nuclear Medicine, Hannover Medical School, Hannover, Germany. ¹³Radcliffe Department of Medicine, University of Oxford and Oxford University Hospitals, Oxford, UK. ¹⁴Department of Biomedical Engineering and Physics, Department of Radiology and Nuclear Medicine, Amsterdam UMC, University of Amsterdam, Amsterdam, Netherlands. ¹⁵Department of Radiology, Erasmus University, Rotterdam, Netherlands. ¹⁶Departments of Biomedical Sciences and Medicine, Cedars-Sinai Medical Center, Los Angeles, CA, USA. ¹⁷Department of Cardiology, Radboud University Medical Center, Nijmegen, Netherlands. ¹⁸Department of Radiology, University Medical Centre Rostock, Rostock, Germany. ¹⁹Centre for Cardiovascular Science, University of Edinburgh, Edinburgh, UK. ²⁰Department of Clinical and Experimental Cardiology and Cardiovascular Sciences, Amsterdam UMC, Heart Center, University of Amsterdam, Amsterdam, Netherlands. ²¹Department of Cardiology, University Medical Center Utrecht, Utrecht, Netherlands. ²²Department of Cardiology, Deutsches Herzzentrum der Charité (DHZC), Charité – Universitätsmedizin Berlin, Berlin, Germany. ²³Division of Cardiology, IRCCS Galeazzi Sant'Ambrogio Hospital, Milan, Italy. ²⁴Department of Nuclear Medicine, Cardiac Imaging, University Hospital Zurich, University of Zurich, Zurich, Switzerland. ²⁵Institute for Biological and Medical Engineering, Pontificia Universidad Católica de Chile, Millennium Institute for Intelligent Healthcare Engineering, Santiago, Chile. ²⁶Deutsches Herzzentrum der Charité (DHZC), Charité – Universitätsmedizin Berlin, Berlin, Germany. ²⁷Berlin Institute of Health, Campus Charité Mitte, Berlin, Germany. ²⁸These authors contributed equally: Aldo J. Vázquez Mézquita, Federico Bivati. ²⁹These authors jointly directed this work: David E. Newby, Marc Dewey.